iScience

CellPress
OPEN ACCESS

Article

Glucocorticoid receptor-mediated *Nr1d1* chromatin circadian misalignment in stress-induced irritable bowel syndrome

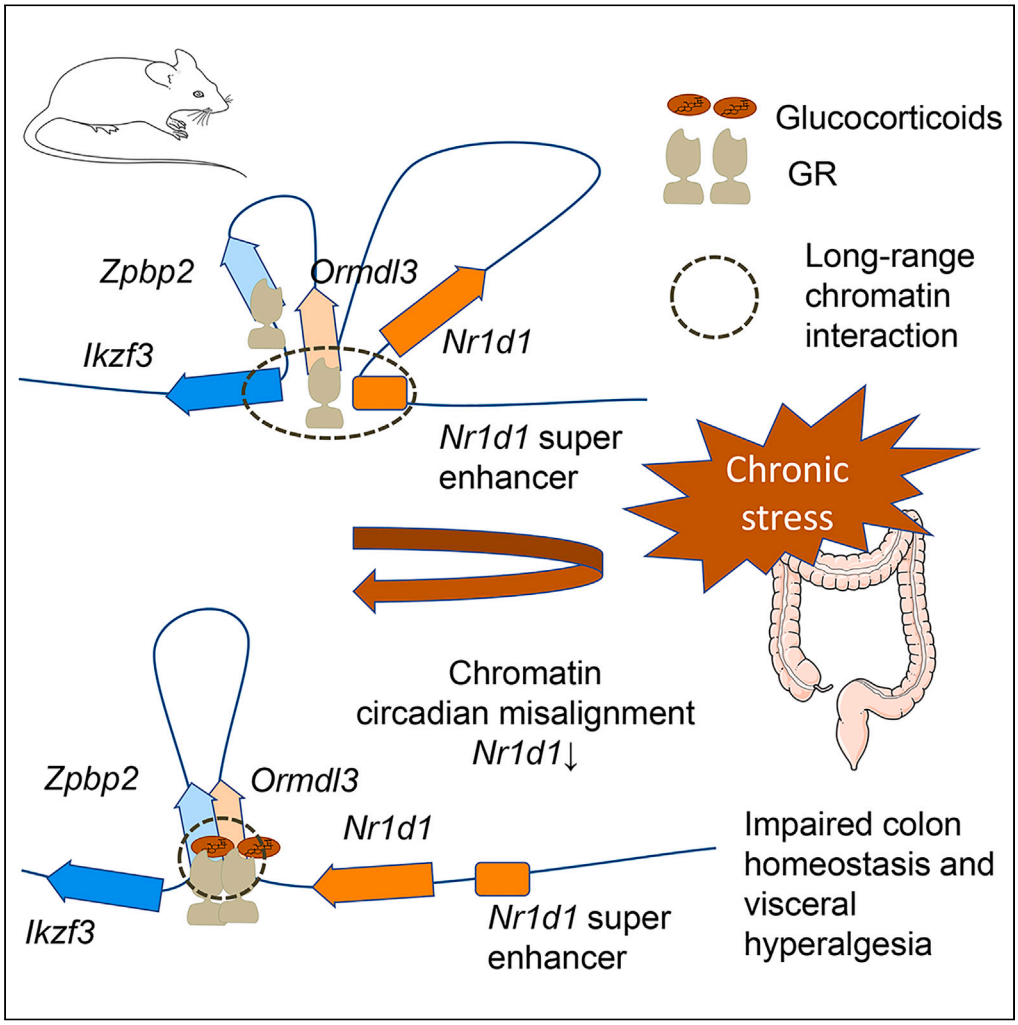

Gen Zheng, Suya Pang, Junbao Wang, ..., John W. Wiley, Xiaohua Hou, Rong Lin

linrong@hust.edu.cn

Highlights

Chronic stress causes chromatin misalignment and impaired colon epithelium homeostasis

Glucocorticoid receptor programs transcriptional changes via chromatin loops

Stress-circadian crosstalk via- Ikzf3-Nr1d1 chromatin suggests translational potential

Zheng et al., iScience *26*, 107137
July 21, 2023
https://doi.org/10.1016/j.isci.2023.107137

iScience

CellPress
OPEN ACCESS

Article

Glucocorticoid receptor-mediated *Nr1d1* chromatin circadian misalignment in stress-induced irritable bowel syndrome

Gen Zheng,[1,9] Suya Pang,[1,9] Junbao Wang,[2] Fangyu Wang,[2] Qi Wang,[3] Lili Yang,[4] Mengdie Ji,[3] Dejian Xie,[5] Shengtao Zhu,[6] Yang Chen,[3] Yan Zhou,[2] Gerald A. Higgins,[7] John W. Wiley,[8] Xiaohua Hou,[1] and Rong Lin[1,10,*]

SUMMARY

Stress-elevated glucocorticoids cause circadian disturbances and gut-brain axis (GBA) disorders, including irritable bowel syndrome (IBS). We hypothesized that the glucocorticoid receptor (GR/NR3C1) might cause chromatin circadian misalignment in the colon epithelium. We observed significantly decreased core circadian gene *Nr1d1* in water avoidance stressed (WAS) BALB/c colon epithelium, like in IBS patients. WAS decreased GR binding at the *Nr1d1* promoter E-box (enhancer box), and GR could suppress *Nr1d1* via this site. Stress also altered GR binding at the E-box sites along the *Ikzf3-Nr1d1* chromatin and remodeled circadian chromatin 3D structures, including *Ikzf3-Nr1d1* super-enhancer, *Dbp*, and *Npas2*. Intestinal deletion of *Nr3c1* specifically abolished these stress-induced transcriptional alternations relevant to IBS phenotypes in BALB/c mice. GR mediated *Ikzf3-Nr1d1* chromatin disease related circadian misalignment in stress-induced IBS animal model. This animal model dataset suggests that regulatory SNPs of human *IKZF3-NR1D1* transcription through conserved chromatin looping have translational potential based on the GR-mediated circadian-stress crosstalk.

INTRODUCTION

Functional bowel disorders (FBDs), including irritable bowel syndrome (IBS), are now recognized as disorders of gut-brain interaction (DGBI), for differential symptoms may share close pathological mechanisms in the gut-brain axis (GBA). Glucocorticoids (GCs) are responsible for the bidirectional interaction of the GBA.[1–3] We previously reported that hypothalamic-pituitary-adrenal (HPA) axis-derived endogenous GCs mediate visceral hyperalgesia and barrier dysfunction of colon intestinal epithelial cells (IECs) in a stress-induced IBS animal model through transcriptional regulation of the glucocorticoid receptor (GR/NR3C1).[4,5] In addition, previous reports of lower *NR1D1* (the core circadian gene encoding REV-ERBα) mRNA levels in IBS patient colonoscopy biopsies led us to propose the existence of a stress-GR-*NR1D1* E-box (enhancer box) pathway as a mechanism for IBS as the basis of this pilot study exploring stress-GR modulated 3D genome structure of IECs.[2,6,7]

The endogenous GCs (cortisol in humans and corticosterone/CORT in rodents) are hormones involved in metabolism, inflammatory responses, cellular proliferation, differentiation, circadian rhythmicity, and stress responses.[2] Furthermore, exogenous GCs have been used as anti-inflammatory steroids that synchronize circadian-dependent chromatin 3D structure and IEC homeostasis *in vitro*.[2,8,9] Ileal-derived CORT regulates the oscillatory circadian-transcriptional network consisting of circadian genes *Per2*, *Clock*, *Arntl* (the gene encoding BMAL1), *Dbp*, and *Nr1d1* in maintaining the homeostasis of IECs in a microbiota-dependent manner through GR.[1,10] CORT levels are elevated in germ-free mice, with GR playing a pivotal role in the downstream transcriptional regulation in GBA.[1,3] Meanwhile, psychological stress elevates blood GCs levels via the HPA axis. GCs bind GR in the cytosol, and GR is translocated to the nucleus, where GR serves as a transcription factor (TF) by binding to glucocorticoid-responsive DNA elements (GREs) in the promoters. This interaction leads to the activation or repression of the transcription of genes involved in the stress responses.[2] The circadian hormone melatonin, which can antagonize GR translocation, may alleviate the effect of stress and demonstrate effectiveness in IBS patients.[11,12] In addition, GR interacts with enhancer GREs and the cohesin loader nipped-B-like protein (NIPBL) to initiate chromatin loop extrusion

[1]Department of Gastroenterology, Union Hospital, Tongji Medical College, Huazhong University of Science and Technology, Wuhan 430022, China

[2]Medical Research Institute at School of Medicine, Wuhan University, Wuhan 430072, China

[3]The State Key Laboratory of Medical Molecular Biology, Department of Biochemistry and Molecular Biology, Institute of Basic Medical Sciences, School of Basic Medicine, Chinese Academy of Medical Sciences and Peking Union Medical College, Beijing 100005, China

[4]Central Laboratory of Yan'an Hospital Affiliated to Kunming Medical University, Kunming Medical University, Kunming 650500, China

[5]Beijing Research Center, Wuhan Frasergen Bioinformatics Co., Ltd, Beijing 100081, China

[6]Key Laboratory of Molecular Biophysics of Ministry of Education, College of Life Science and Technology, Huazhong University of Science and Technology, Wuhan 430074, China

[7]Department of Computational Medicine and Bioinformatics, Medical School, University of Michigan, Ann Arbor 48109, MI, USA

[8]Department of Internal Medicine, Medical School, University of Michigan, Ann Arbor 48109, MI, USA

[9]These authors contributed equally

[10]Lead contact

*Correspondence: linrong@hust.edu.cn

https://doi.org/10.1016/j.isci.2023.107137

as a mechanism for long-distance regulation: GR and NIPBL bind enhancer GREs firstly and load cohesin ring to guide the formation of chromatin loop, then the chromatin slides through the cohesin ring until the formation of stable transcription-regulatory enhancer-promoter interaction via the TF binding DNA elements.[13] E-box is a DNA response element targeted by the CLOCK:BMAL1 TF complex in the circadian transcriptional network.[14,15] GR also interacts indirectly with E-boxes in the *Nr1d1* promoter via the CLOCK:BMAL1 protein complex to repress *Nr1d1* during stress.[7] Intestinal deletion of *Nr1d1* demonstrated that NR1D1 is a crucial regulator of the transcriptome in the mouse colitis (inflammatory bowel disease [IBD]) model; loss of NR1D1 leads to increased colonic inflammation through NLRP3.[16] The NLRP3 inflammasome is also an emerging therapeutic target for chronic pain and IBS.[17] Moreover, diurnal dynamic interactions between GR and NR1D1 protein modulate their nuclear co-localization by co-binding to the genomic DNA, thereby regulating downstream transcription and NR1D1 coupled GC genomic action.[18,19] GR and NR1D1 interact with the NCOR1 (nuclear receptor corepressor 1)-HDAC3 (histone deacetylase 3) complex and mediate GC and circadian-driven chromatin looping, thereby suggesting circadian-stress 4D nucleome (4DN/spatial and temporal changes in the structure of the nucleus) crosstalk.[20,21] During the circadian, 5′ *Fbxl20* to 3′ *Nr1d1* super-enhancer circadian oscillatory chromatin looping was regulated by the BMAL1, NR1D1, and cohesin-CTCF.[22] GR may participate in this regulation, and stress may reprogram the *Nr1d1* chromatin in 3D.[13–15]

Chromatin 3D structures, including long-distance enhancer-promoter interactions, can help elucidate the pathological mechanism of single nucleotide polymorphisms (SNPs): Most SNPs are located in non-coding areas and so, might serve as enhancers. The PsychENCODE project studying these enhancer-promoter pairs identified NR1D1 as a "master regulator" of targetable transcriptional networks.[23] Specifically, regulatory SNPs located in long-range enhancers of differentially expressed GR target genes could predict stress-induced risk-related brain function and psychiatric disorders as well as metabolic effects of GC and GC treatment responses.[24,25] Since the workshop "Functional Bowel Disorders: A Roadmap to Guide the Next Generation of Research," high-quality multi-omics data, including transcriptomic and genome-wide association studies (GWAS) of IBS patients, were generated.[26–31] However, IBS-related chromatin 3D structure remains elusive.[2,23] The latest GWAS of a large IBS population revealed IBS risk loci and SNPs that suggested shared genetic pathways with psychological mood and anxiety disorders; *NIPBL* was detected in IBS etiology analysis (shown in Supplementary Table 10 of this reference).[30] The GR-NIPBL-cohesin target gene *TSC22D3* (*GILZ*/glucocorticoid-induced leucine zipper protein) was the most significant differentially expressed gene (DEG) between IBS-C (constipation) and IBS-D (diarrhea) (false discovery rate (FDR) < 0.005, shown in Table S6 of this reference).[13,29] The transcriptional regulation mediated by GR-NIPBL-cohesin is responsible for the response to GC and may also participate in stress-induced IBS.[13,32] Capture-C sequencing of human hypothalamic-like neurons and colonoids 3D genomes were performed to explore stress and depression-associated IBD; *STARD3* at the 5′-distal region of *NR1D1* and the IBS DEG *CDH3* (P-cadherin) (IBS-C vs. Healthy Control, FDR <0.05) were identified as putative effector genes.[27–29,33] This study also revealed a close genetic correlation between depression with IBD and asthma.[33] Encoded between *STARD3-NR1D1*, the hypothesized IBS DEG *ORMDL3* shares the IBS SNP rs2872507 with *IKZF3*, a recently verified IBS DEG with the highest significance (IBS-C vs. IBS-D, right colon $p < 0.00001$ left colon $p < 0.0000001$; IBS-D vs. Healthy Control right colon $p < 0.01$ left colon $p < 0.0001$).[27,28,31] This SNP also regulates IBD DEGs encoded within the conserved 17q12-q21 *ERBB2* (*HER2*)-*GRB7-IKZF3-ZPBP2-GSDMB-ORDML3-MED24* chromatin region upstream of *NR1D1* and is associated with differential responses to GC therapy against asthma.[34–36] The asthma-risk variants rs4065275 (*ORMDL3* site) and rs12936231 (*ZPBP2* site) switch CTCF-binding sites that mediate pathological *IKZF3-ORMDL3* to *ZPBP2-ORMDL3* chromatin loop changes.[37] Thus, the 5′ *ZPBP2-ORMDL3* region regulates 3′ *NR1D1* circadian transcription *in cis* from long distances.[35] The potential GR-mediated chromatin interactions linking these regulatory SNPs have translational potential in precision medicine against psychological mood and anxiety disorders and IBS.[2,23,30] *In vitro* germ-free colonoids used in the Capture-C sequencing study tend to lose circadian oscillatory transcription without daily GC treatments; it has limitations in studying intestinal epithelium *Nr1d1* regulated by circadian and microbiota *in vivo*.[1,9,33,38] To overcome this limitation, we employed a validated water avoidance stressed (WAS) mouse model of IBS to explore 3D genome structure *in vivo*.[2] BALB/c strain used in this study is the preferred strain for circadian-stress crosstalk.[39]

RESULTS

Stress altered circadian-related transcription responsible for IBS phenotype

We first performed a transcriptomic analysis to identify DEGs responsible for colonic stress responses (Figures 1 and S1). Decreased mRNA levels of *Nr1d1* and the NR1D1 downstream clock gene target *Dbp* were the most

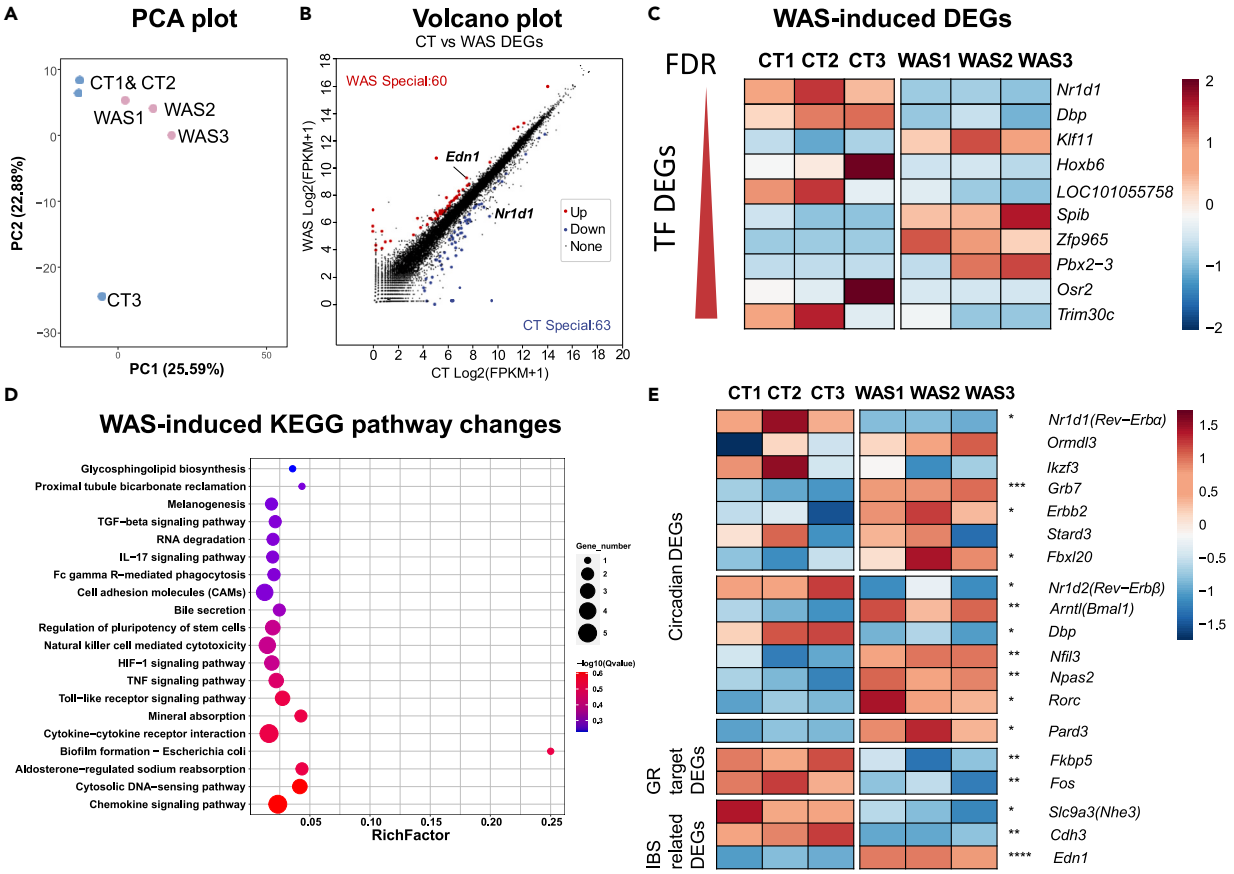

F BART analysis of WAS-induced DEGs for transcription regulators

Transcription factors

NR3C1 RXRA HNF4A **AR** FOXA1

FOXA2 ELF5 NFIB **ESR1** STAT5A

NR1H2 STAT5B BCL6 ONECUT1

PROX1 **CRY2** PPARA HNF4G **PER2**

TCF7L1 PTF1A NKX3-1 AHR HNF1B

CRY1 NR1D1 NR1D2 BHLHA15 MYOD1

TCF4 **NFIL3 PER1** ASCL1 THRB MYOG

Circadian gene TFs

Chromatin regulators

HDAC3 SMC1A CTCF SMC3 RAD21

EZH2 SUZ12 JARID2 CBX7 **STAG1**

PCGF6 BMI1 NCOR2 PCGF2 SRC

Cohesin components

G Cytoscape analysis for transcription regulatory network

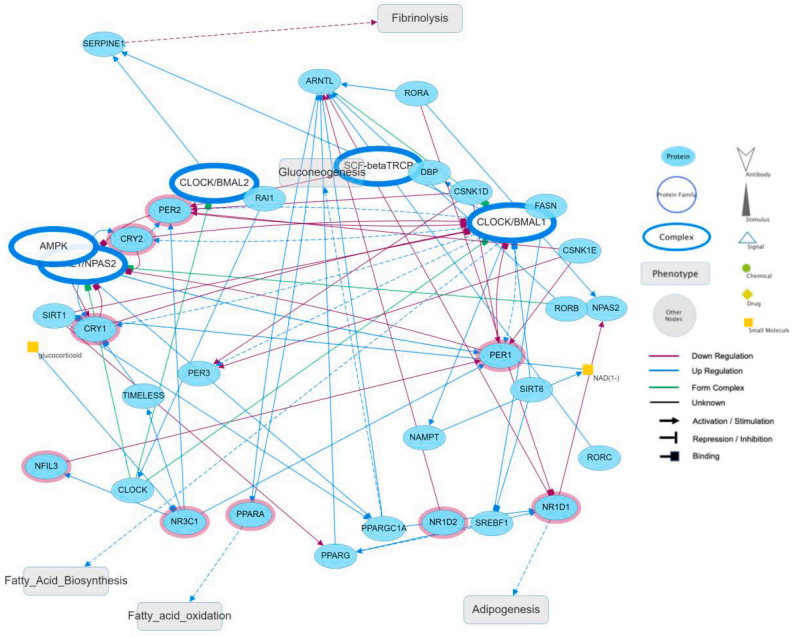

Figure 1. Stress-induced colon epithelium DEGs suggest circadian-stress crosstalk

Control (CT) and water avoidance stressed (WAS) BALB/c mouse colon epithelium cells were isolated for RNA-seq analysis.

(A) Principal component analysis.

(B) Volcano plot of DEGs.

(C) Heatmap of transcription factor DEGs.

(D) KEGG pathway enrichment of WAS-induced DEGs.

(E) Heatmap of circadian, GR target, and IBS-related DEGs. Statistical significance was determined using an unpaired *t* test with Welch's correction (*, $p < 0.05$; **, $p < 0.01$; ***, $p < 0.001$; ****, $p < 0.0001$; N = 3).

(F) BART (binding analysis for regulation of transcription) analysis of WAS-induced DEGs for potential transcription regulators.

(G)The top 50 transcription regulators were analyzed with Cytoscape, and the circadian clock was identified as the potential stress-modulated transcription network with the highest similarity.

significant DEGs that encode TFs (Figures 1A and 1C). The KEGG (Kyoto Encyclopedia of Genes and Genomes) pathway enrichment analysis enriched chemokine signaling, tumor necrosis factor (TNF), and bile acid secretion changes (Figure 1D). Given the emerging evidence of circadian gene *Nr1d1* and *Dbp* in intestinal circadian misalignment impaired intestinal homeostasis, we focused our investigations on these genes.[10,14,16,38,40] In our hypothesis-driven analysis, we *t* tested our interested circadian and IBS-related genes for low-amplitude changes, which were filtered by automated RNA-seq analysis with a 2-fold threshold. In addition to IBS and IBD-related DEGs encoded within the conserved *Nr1d1-Ormdl3-Ikzf3-Grb7-Erbb2-Stard3-Fbxl20* chromatin, we observed stress responses in the validated circadian chromatin 3D structure-regulated genes *Nr1d2*, *Npas2*, *Rorc*, and *Pard3*.[8,21,22,31,35,41,42] NR1D1 downstream circadian gene *Arntl*(*Bmal1*), *Nfil3* elevated.[16] IBS therapeutic target homolog *Slc9a3* (hydrogen exchanger 3/*Nhe3*) decreased.[43] IBS-related GR target genes *Fkbp5* and *Fos* decreased.[3,13,31] IBS DEG homolog *Cdh3* increased.[29] Elevated *Edn1* was identified as an IBS-related DEG with high significance (Figures 1B and 1E).[44] We employed BART (binding analysis for regulation of transcription) for potential transcription regulators of WAS-induced DEGs. Within the predicted transcriptional regulators, GR/NR3C1 was the most significant TF and HDAC3 was the most significant chromatin regulator (Figure 1F). Cohesin components SMC1A, SMC3, RAD21, STAG1, and CTCF involved in the GR-mediated promoter-enhancer interaction were also recognized.[13] We then predicted the potential transcription network with the most significant 50 transcription regulators from BART analysis and identified the circadian clock as the most similar pathway using Cytoscape; GC can modulate this transcriptional network via GR (Figure 1G). Then we examined downstream circadian disturbances in colon epithelial cells via qPCR at ZT2-ZT26; stress altered the circadian expression of circadian genes and significantly increased *Cry1*, which is repressed by NR1D1 through NR1D1-mediated enhancer-promoter chromatin looping (Figure S2).[21] The transcriptome results were confirmed by Western blot analysis showing decreases in levels of NR1D1 and GR and increased expression of the NR1D1-mediated inflammatory proteins NLRP3, IL1β, and IL6.[5,16] In addition, intestinal barrier regulator PARD3 decreased (Figure 2A).[45] Furthermore, WAS-induced IBS phenotype, including inflammatory infiltration, barrier dysfunction, and visceral hyperalgesia, were verified. Injections of NR1D1 agonist SR9009 during water avoidance stress significantly prevented these phenotype changes (Figures 2B–2F).[16,46] We also evaluated the stress-induced anxiety behavior via the open field test; WAS significantly increased velocity and total distances (Figure S3).[47] These findings indicate that WAS BALB/c mice mimic hypothesized stress-GC-GR-NR1D1 IBS pathology and confirm the suitability of this model for further analysis (Figures 1 and 2).[2]

GR repressed *Nr1d1* via promoter transcription start site E-box

Given that GR is potentially the most significant transcription regulator of WAS-induced transcriptomic responses, we used the highly sensitive CUT&Tag sequencing method to profile genomic GR binding of colonic IECs (Figure 1F). The GR binding peaked at transcription start sites (TSSs) (Figure 3A). WAS caused 33% GR binding changes in promoters, 34% in introns, and 25% in the distal intergenic region (Figure 3B). The changes in the TNF signaling pathway and melanogenesis in KEGG analysis were consistent with transcriptome (Figures 1D and 3C). Specifically, WAS induced a gap in GR binding around the *Nr1d1* promoter E-box (Figure 3D). This TSS E-box CpG was 1% methylated in stressed mice, which may have caused the observed gap by blocking the TF binding site (Figure 3E). Within mouse colon crypts derived young adult mouse colon (YAMC) cells, we verified the stress-GC-GR-*Nr1d1* promoter E-box pathway responsible for *Nr1d1* repression via luciferase assays (Figures 3F and 3G).[2,7] In addition, we verified GC's repression of NR1D1 protein *in vitro*: NR1D1 was downregulated by CORT, and GR antagonist RU486 prevented this effect. Furthermore, NR1D1 decrease-related elevation in NLRP3 and IL1β was reproduced by CORT treatment and could be prevented by NR1D1 agonist SR9009. These data support a stress-GC-GR-NR1D1-NLRP3 inflammasome pathway in stress-impaired colon epithelium homeostasis (Figure 3H).[2,7,16,17]

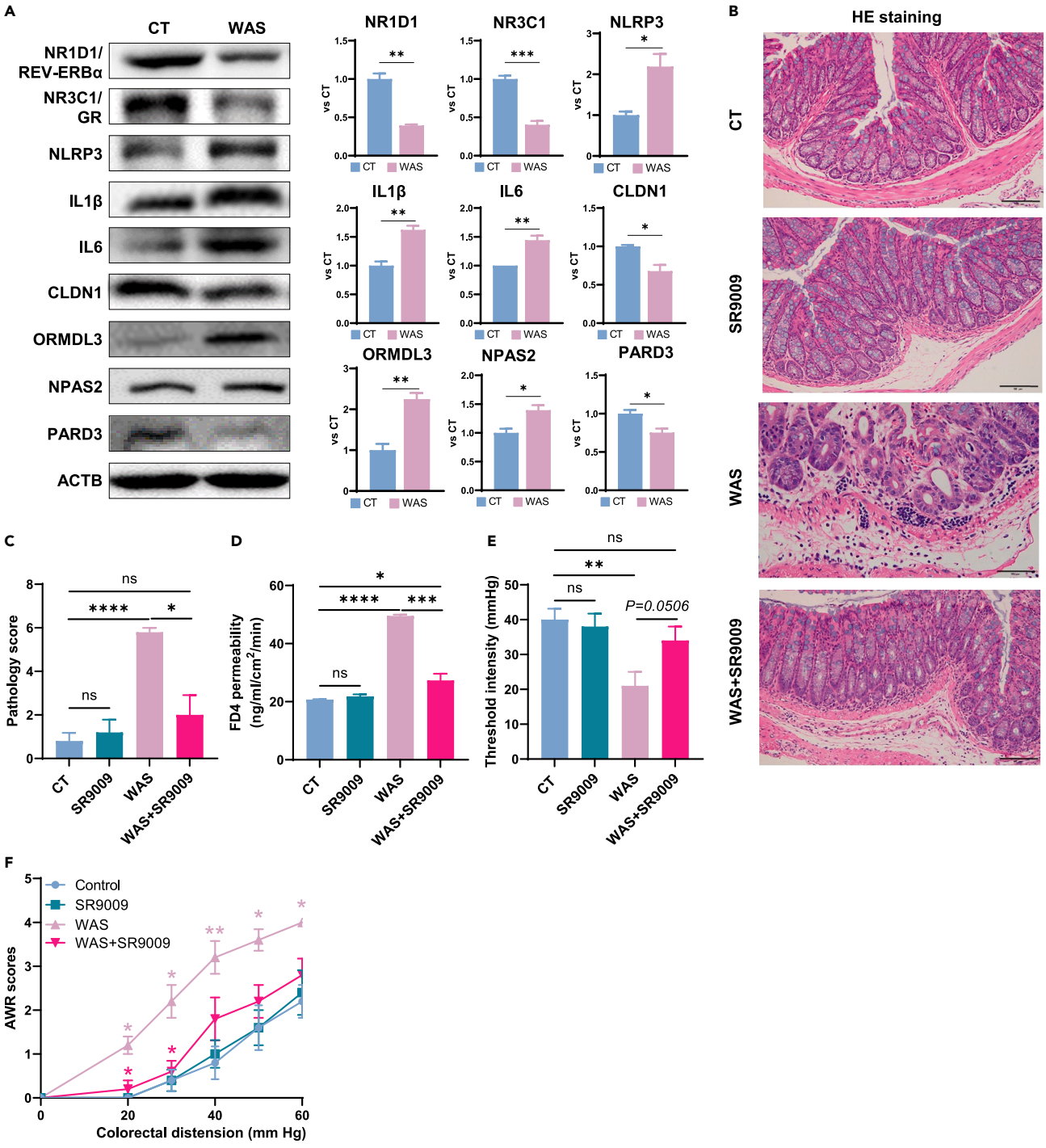

Figure 2. The WAS-induced transcriptome changes correlated with IBS phenotypes

(A) Western blot analysis of control (CT) and water avoidance stressed (WAS) mouse colon IECs.

(B) Typical hematoxylin-eosin (HE) staining of CT and WAS colon epithelium with/without NR1D1 agonist SR9009 intervention. Inflammatory infiltration was present in WAS mice, and SR9009 significantly prevented morphology changes.

(C) Pathology scores increased in WAS mice, and SR9009 prevented this effect.

(D) Stress increased FD4 (fluorescein isothiocyanate-dextran 4 kDa) permeability, and this effect was antagonized by SR9009 intervention.

(E) Stress reduced the thresholds of pain responses. Data are expressed as means ± standard error, and statistical significance between groups was determined using an unpaired *t* test with Welch's correction (*, $p < 0.05$; **, $p < 0.01$; ***, $p < 0.001$; N = 3, 4, 5).

(F) Visceral hyperalgesia was evaluated with AWR (abdominal withdrawal reflex) scores in response to CRD (colorectal distension). AWR data were analyzed with two-way ANOVA analysis (with Tukey's multiple comparison test); the significance between WAS/CT and WAS+SR9009/WAS is illustrated (*, $p < 0.05$; **, $p < 0.01$; N = 4, 5).

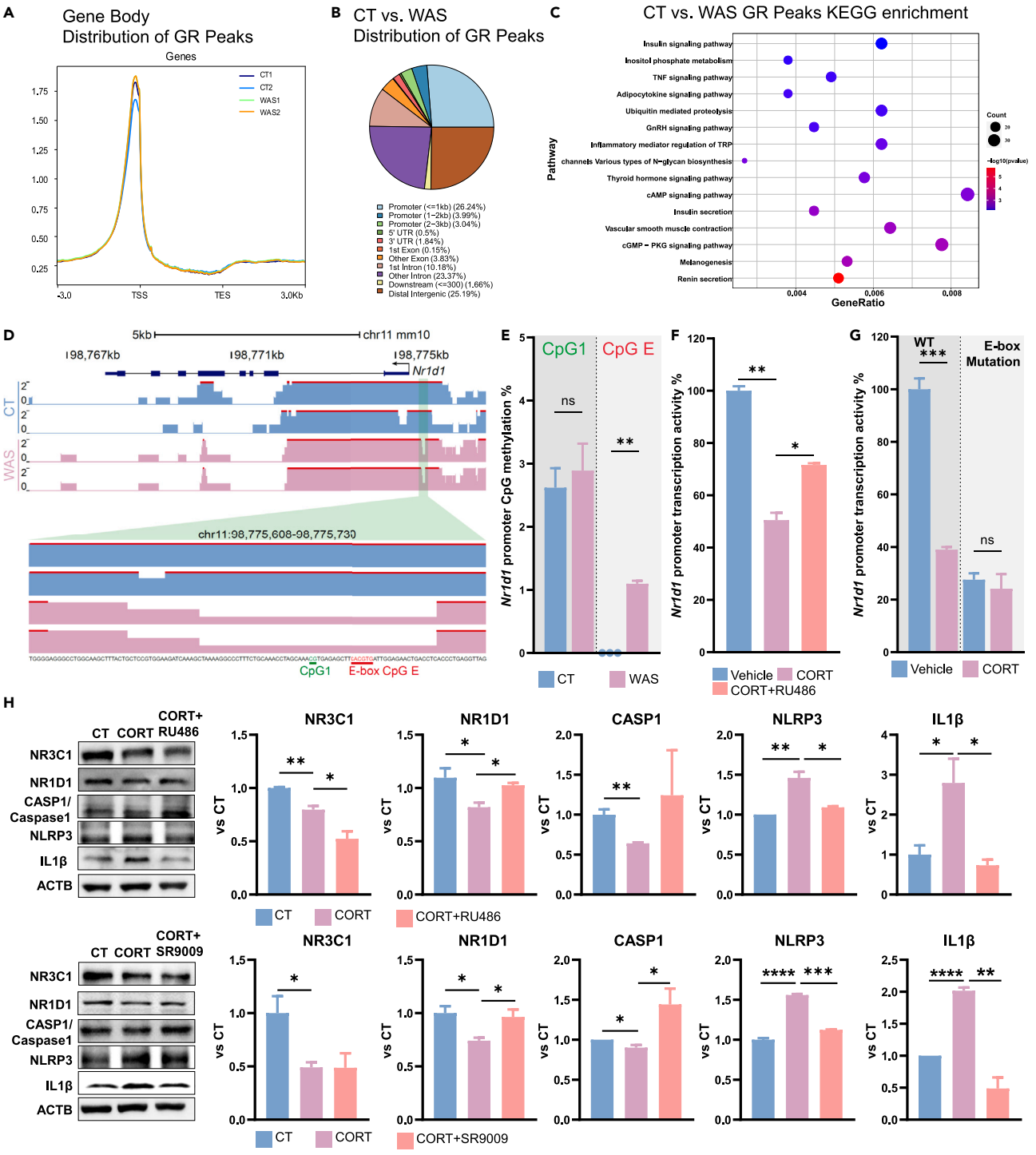

Figure 3. Stress-induced GR binding change at *Nr1d1* TSS E-box

Control (CT) and water avoidance stressed (WAS) mouse colon epithelium cells were isolated for CUT&Tag analysis; hypothesis-free analysis of GR cistrome.

(A) Gene body.

(B) Differential peak annotation.

(C) KEGG pathway enrichment of differential peaks.

(D) Each lane represents IECs pooled from four mice, stress reduced GR binding at the E-box (CACGTG) upstream of the *Nr1d1* TSS.

(E) Pyrosequencing analysis of the genomic DNA CpGs within the gap in GR binding around the E-box.

Figure 3. *Continued*

(F and G) *Nr1d1* promoter activity in differentiated mouse colon epithelium YAMC cells. 1 μM CORT treatment repressed *Nr1d1* transcription, and the GR antagonist RU486 ameliorated this effect. *Nr1d1* promoter TSS E-box mutation reduced *Nr1d1* transcription.

(H) Western blot analysis of YAMC cells treated with CORT, RU486, and NR1D1 agonist SR9009. Data are expressed as means ± standard error. Statistical significance was determined using an unpaired *t* test with Welch's correction (*, $p < 0.05$; **, $p < 0.01$; ***, $p < 0.01$; ****, $p < 0.0001$; N = 3).

GR remodeled *Ikzf3-Nr1d1* circadian chromatin loops between GR-bound E-box sites

Within our conserved target region of interest (*Ikzf3-Nr1d1*), bidirectional *Ikzf3*(3′–5′)-*Zpbp2* (5′–3′), *Ormdl3*, and *Nr1d1* promoters have conserved E-boxes. GR binding at these promoters and the WAS-induced *Ikzf3-Zpbp2* promoter E-box GR peak suggest long-range regulation in addition to the promoter activity (Figure 4A).[35] To clarify the effect of stress on chromatin 3D structures, we employed a high-accuracy BL-Hi-C method.[48] Furthermore, we compared the chromatin 3D structures with transcriptome and GR cistrome data. In this region, we found that the WAS-induced *Zpbp2-Ormdl3* chromatin loop replaced the *Ikzf3-Ormdl3* and *Ormdl3-Nr1d1* super-enhancer loops in control at the chromatin looping sites that include the GR bound *Ikzf3-Zpbp2* bidirectional promoter and *Nr1d1* super-enhancer.[22,35] In addition, WAS elevated *Nr1d1* super-enhancer GR binding (Figure 4B). This pattern correlates with IBS and IBD SNP rs2872507 regulates transcription of this region and IBD SNP (rs12936231) mediated long-range regulation of *NR1D1* via the formation of IBD-related *ZPBP2-ORMDL3* loop (Figures 4C and 4D).[27,35–37] Moreover, WAS-induced 5′ distal *Fbxl20-Ormdl3* and *Ppp1r1b-Ormdl3* loops between the circadian *Nr1d1* super-enhancer interactome sites replaced the *Stard3-Ormdl3* loop in control (Figure S4).[22,42] These data suggest that GR reprogrammed *Ikzf3-Nr1d1* circadian controlled chromatin in response to the stress, formation of conserved pathological *Zpbp2-Ormdl3* loop abolished *Ormdl3-Nr1d1* super-enhancer loop, which participated *Nr1d1* circadian transcription.[22]

Stress altered circadian-regulated, GR-regulated, and IBS-related chromatin 3D structures

In addition to *Nr1d1*, WAS also altered other circadian-regulated 3D chromatin architectures, including the clock gene *Dbp*, the circadian chromatin hub gene *Pard3*, and the Nr1d1/Rev-erbα regulated clock gene *Npas2* (Figures 5A–5C).[15] Dbp locus displayed increased chromatin clustering close to the *Dbp* gene, correlating with decreased transcription (Figure 5A).[8,10,14] In addition, we observed WAS-induced *Pard3* chromatin loop changes correlating with GR binding (Figure 5B).[15,41] Stress also altered NR1D1-regulated Npas2 circadian chromatin loops and increased *Npas2* promoter GR binding relevant to increased *Npas2* expression (Figure 5C).[16,21] These data further elucidated the 3D chromatin structures of GR-mediated circadian misalignment in addition to the stress-disturbed *Ikzf3-Nr1d1* chromatin looping, which disturbed the circadian transcription network (Figures 1G and 4).[2,10,14] Furthermore, we analyzed stress-transformed 3D chromatin architectures of GR target genes. IBS-related *Fkbp5* exhibited a stress-elevated stripe-like structure that correlated with GR binding peak and decreased transcription, similar to GR-NIPBL mediated long-range regulation (Figure 5D).[13,49] IBS DEG *CDH3* 3D structure is likely involved in stress-impaired colon homeostasis.[29,33] We observed stress-induced GR binding changes around *Cdh3* and altered *Cdh3-Cdh1* chromatin structure targeted by GR that were consistent with the transcription pattern (Figures 1E and 5E). These chromatin 3D structure changes suggest the existence of stress-GR transcriptional programming in IBS at multiple conserved genomic loci.[2]

Stress-induced GR transcriptional regulation is validated by intestinal deletion of *Nr3c1*

Having established the role of GR in transcriptional regulation of the IECs, we next validated this in an *in vivo* model by generating BALB/c *Nr3c1*$^{\triangle IEC}$ conditional knockout mice according to the protocol used with C57BL/6J background.[50] In the PC analysis of RNA-seq, *Nr3c1*$^{\triangle IEC}$ mice exhibited a closer correlation between CT and WAS groups, with fewer DEGs in the volcano plot and altered KEGG pathway enrichment (Figures 6A–6C). Within the TF DEGs, *Nr3c1* deletion changed the expression of steroid-responding transcription factors, including decreased *Nr3c1* levels and upregulation of the estrogen receptors *Esr1* and *Esrrg*. Stress elevated *Esr1* and *Esrrg* mRNA levels in *Nr3c1*$^{fl/fl}$, but not in *Nr3c1*$^{\triangle IEC}$ mice. WAS elevated *Egr1* in *Nr3c1*$^{fl/fl}$ mice. IBS-related TF genes *Nfkbiz, Irf7*, and *Prdm1* were detected as shared TF DEGs of stressed *Nr3c1*$^{fl/fl}$ and *Nr3c1*$^{\triangle IEC}$ mice; *Ikzf1* and *Ikzf3* were detected as WAS-induced DEG in *Nr3c1*$^{\triangle IEC}$ mice.[27,28,31,51] *Nr3c1* is the only TF DEG between stressed *Nr3c1*$^{fl/fl}$ and *Nr3c1*$^{\triangle IEC}$ mice, supporting GR as the key regulator of the stress-modulated transcription network (Figures 1F, 1G, and 7D). In accordance with the predicted transcription regulatory network, the deletion of *Nr3c1* altered the transcription of the circadian TF genes *Per2, Per3, Id2, Tef, Arntl/Bmal1, Dbp*, and *Rorc* (Figures 1G, 6D, and 6E). This pattern and GR binding along these TF genes supported the pivotal role of GR in stress-induced transcriptional re-programming, which involves the circadian

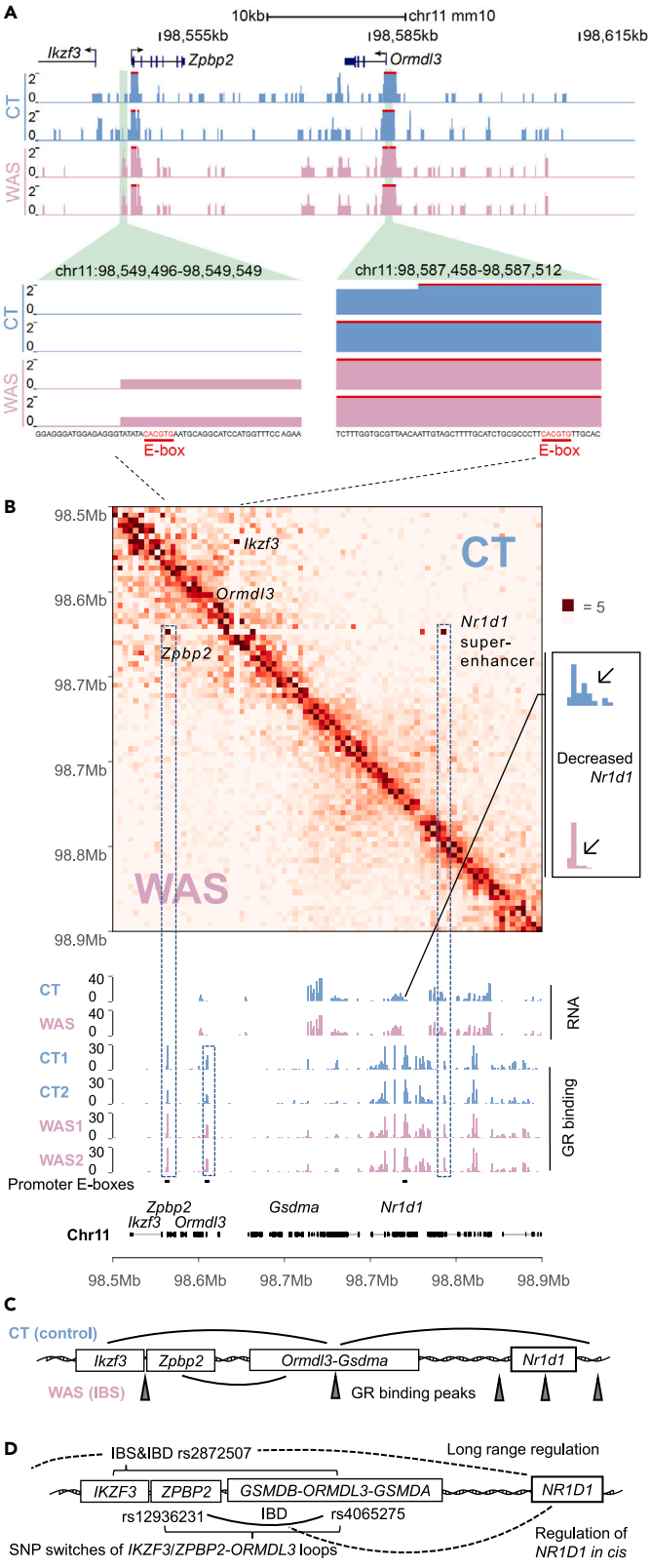
A
10kb
chr11 mm10
98,555kb
98,585kb
98,615kb
Ikzf3
Zpbp2
Ormdl3
CT
WAS
chr11:98,549,496-98,549,549
chr11:98,587,458-98,587,512
E-box
E-box
B
98.5Mb
98.6Mb
98.7Mb
98.7Mb
98.8Mb
98.9Mb
Ikzf3
Ormdl3
Zpbp2
CT
WAS
Nr1d1
super-
enhancer
= 5
Decreased
Nr1d1
CT
WAS
CT1
CT2
WAS1
WAS2
RNA
GR binding
Promoter E-boxes
Zpbp2
Ikzf3
Ormdl3
Gsdma
Nr1d1
Chr11
98.5Mb
98.6Mb
98.7Mb
98.7Mb
98.8Mb
98.9Mb
C
CT (control)
Ikzf3
Zpbp2
Ormdl3-Gsdma
Nr1d1
WAS (IBS)
GR binding peaks
D
IBS&IBD rs2872507
Long range regulation
IKZF3
ZPBP2
GSMDB-ORMDL3-GSMDA
NR1D1
rs12936231
IBD
rs4065275
SNP switches of IKZF3/ZPBP2-ORMDL3 loops
Regulation of
NR1D1 in cis

Figure 4. Stress-induced *Ikzf3-Zpbp2-Ormdl3-Nr1d1* circadian chromatin loop misalignment

(A and B) BL-Hi-C was performed with colon IECs isolated from two control (CT) and two water avoidance stressed (WAS) BALB/c mice; data from each group were combined for visualization; each RNA track represents the combined RNA-seq data from three mice; GR-CUT&Tag tracks are also shown.

(C) The stress-induced *Zpbp2-Ormdl3* loop replaced the *Ikzf3-Ormdl3* & *Ormdl3-Nr1d1* super-enhancer in control.

(D) This region is conserved with human *IKZF3-ZPBP2-ORMDL3-NR1D1* chromatin, with disease-risk SNPs causing switching of the *IKZF3-ORMDL3*/*ZPBP2-ORMDL3* chromatin loops to mediate long-range regulation of *NR1D1* transcription.

transcription network (Figures 1F, 1G, and S5).[2] In our hypothesis-driven analysis, *Nr3c2* (mineral corticoid receptor/*MR*, GC's alternative receptor) was upregulated in *Nr3c1*$^{\Delta IEC}$ mice as potential compensation for GR loss. Furthermore, chronic stress repressed *Nr3c2* in *Nr3c1*$^{\Delta IEC}$ mice (Figure 6E). Notably, the deletion of *Nr3c1* partially reversed the wild-type (WT) DEG pattern of the *Nr1d1-Ikzf3-Grb7-Erbb2* chromatin that we had observed in the WT mice (Figures 1E, 4, 6E, and S4).

Western blotting revealed that *Nr3c1* deletion tended to reverse the WAS-induced changes in NR1D1, NLRP3, IL1β, CDH1, CDH3, and ORMDL3 protein levels (Figure 7A). *Nr3c1* knockout also reduced the significance of stress-induced changes in NR1D1, NLRP3, IL1β, IL6, CLDN1, NPAS2, CDH1, and CDH3 expression, which are responsible for impaired intestinal homeostasis (Figures 2A and 7A).[5,16] The stress-GR-NR1D1-NLRP3 inflammasome pathway is further confirmed (Figures 2, 3, and 7).[2,16] Deletion of *Nr3c1* in BALB/c impaired the colon epithelium barrier function and homeostasis, similar to the effects observed on the C57BL/6J background (Figures 7B–7E).[50] WAS caused less permeability change in the *Nr3c1*$^{\Delta IEC}$ mice than in *Nr3c1*$^{fl/fl}$ mice, correlating with *Nr3c1* deletion prevented WAS-induced barrier function protein CLDN1, CDH1, and CDH3 decreases (Figures 7A–7E). BALB/c *Nr3c1*$^{fl/fl}$ mice had lower pain threshold than WT mice, possibly due to the side effects of tamoxifen injections, which cause pain (Figures 2E and 7F). Although two-way ANOVA analysis did not detect significant differences between the *Nr3c1*$^{fl/fl}$ CT and WAS mice, significantly increased pain responses were detected between *Nr3c1*$^{fl/fl}$ CT/*Nr3c1*$^{\Delta IEC}$ WAS and *Nr3c1*$^{\Delta IEC}$ CT/*Nr3c1*$^{\Delta IEC}$ WAS groups (Figures 7F and 7G). These results correlated with the stress-induced "vascular smooth muscle contraction" pathway changes detected in *Nr3c1*$^{fl/fl}$ mice regulated by GR binding (Figures 3C and 6C). These protein level changes correlating with IBS phenotypes supported GR's transcriptional programming in stress-induced IBS (Figures 6 and 7).[2,50] We compared published human IBS transcriptome, GWAS, and 3D genomic GBA mapping data with animal dataset generated in this study and found a potential conserved GR mediated *Ikzf3-Nr1d1* chromatin circadian misalignment responsible for IBS phenotypes of colonic inflammation and increased permeability and visceral hyperalgesia (Figure S6).

DISCUSSION

In this study, we provided the first evidence of chromatin 3D structure changes in the stress-induced IBS animal model, a significant advance from previous knowledge of epigenetics.[14,32,52] This proof-of-concept study suggests that this novel GR-mediated circadian-stress crosstalk in the 3D genome contributes to the IBS-related transcription changes, especially at the conserved *Ikzf3-Nr1d1* chromatin regulated by TFs GR, BMAL1, and NR1D1, and chromatin regulators HDAC3, cohesin, and CTCF (Figure S6).[13,22,38] Circadian programming of this *Nr1d1* chromatin by chromatin remodeler HDAC3 controls diurnal rhythms of the host intestinal metabolism in a microbiota-dependent manner.[38] Alteration in *Nr1d1* transcription at ZT0 may cause downstream increased *Cry1* transcription, which is repressed by NR1D1-mediated enhancer-promoter looping; these findings supported our original hypothesis (Figure 1 and S2).[2,21] It can be speculated that prolonged WAS-induced circadian misalignment may contribute to dysbiosis and colitis.[14,20,53] These mouse model findings consistent with human data suggest a conserved synergy of GR, BMAL1, HDAC3, and cohesin-CTCF regulate *IKZF3-NR1D1* chromatin looping[7,13,14,18,19,22] (Figure S6B). Since this chromatin region is epigenetically programmed by intestinal microbiota, personalized probiotics based on *IKZF3-NR1D1* SNPs and differential *IKZF3* levels in subtypes of IBS could be a potential intervention against the pathological chromatin circadian misalignment[31,35,38] (Figure 4D). The potential stress-GR-NR1D1-NLRP3 inflammasome IBS pathology pathway identified in this study could be intervened by the circadian hormone melatonin treatment.[40,54,55] Barrier function gene *PARD3* has IBS SNPs.[45,56] *PARD3* is positioned diurnally to the H3K9me2 repressive nuclear lamina-associated domains in human colon epithelial HCT116 cells.[41,45] We detected *Pard3* promoter methylation and repressed transcription in our parallel WAS rat study.[57] Mouse data in this study provided further evidence suggesting the stress-disturbed circadian regulation of *Pard3* (Figure 5B). The IBS-related *CDH3*(P-cadherin)-*CDH1*(E-cadherin) chromatin encodes genes responsible for colon barrier function and homeostasis.[9,27,29,33] *Cdh3* and *Cdh1* are also

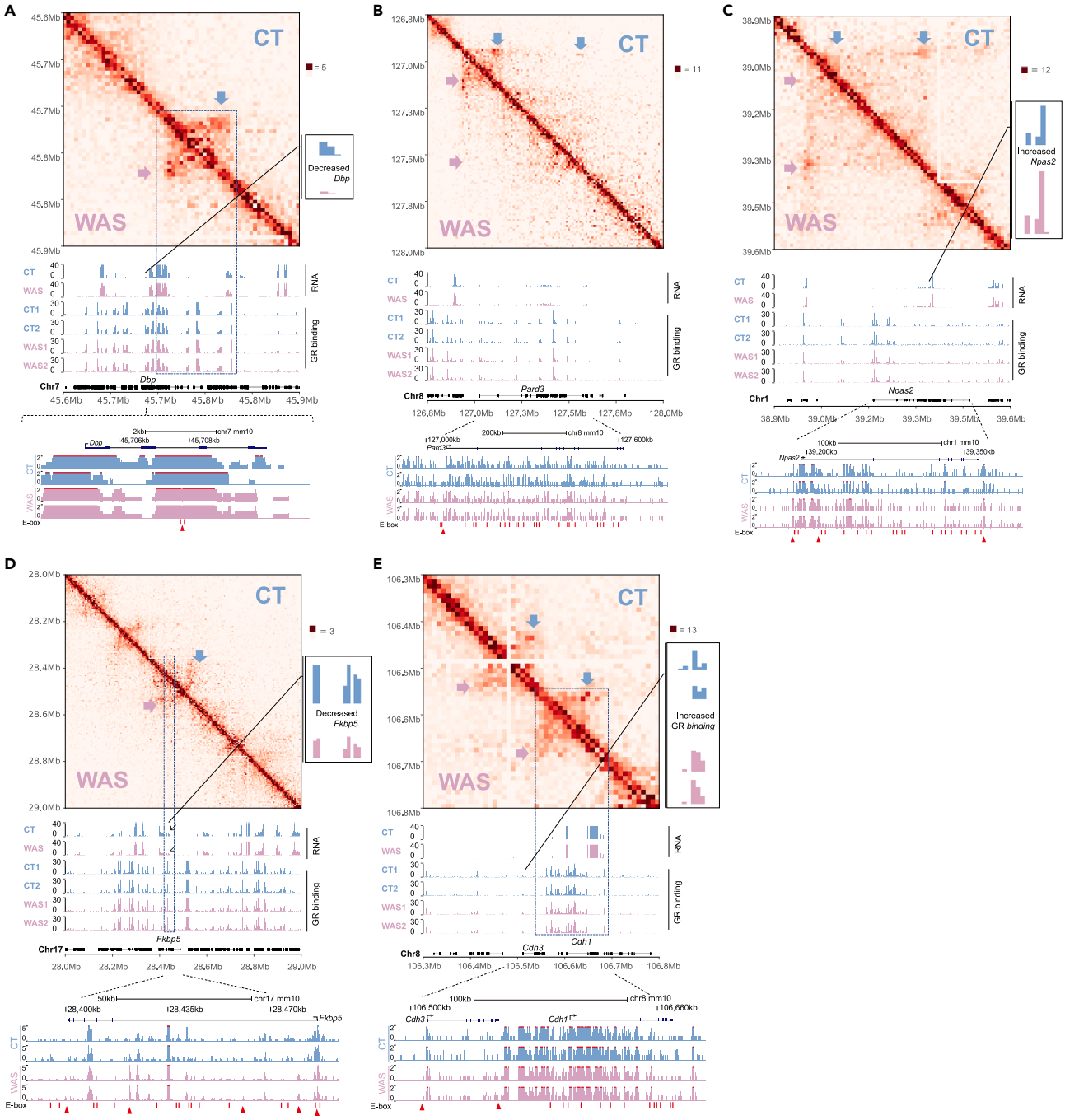

Figure 5. Stress altered circadian-regulated, GR-regulated, and IBS-related chromatin 3D structures

BL-Hi-C was performed with colon IECs isolated from two control (CT) and two water avoidance stressed (WAS) BALB/c mice; data from each group were combined for visualization; each RNA track represents the combined RNA-seq data from three mice; GR-CUT&Tag tracks are also shown. E-boxes (CACGTG) and differential GR binding are marked.

(A) Circadian gene *Dbp* chromatin.

(B) Circadian chromatin hub *Pard3*.

(C) The NR1D1 target circadian gene *Npas2*.

(D) GR target gene *Fkbp5* stripe-like structure.

(E) IBS-related *Cdh3* (P-cadherin)-*Cdh1* (E-cadherin) chromatin.

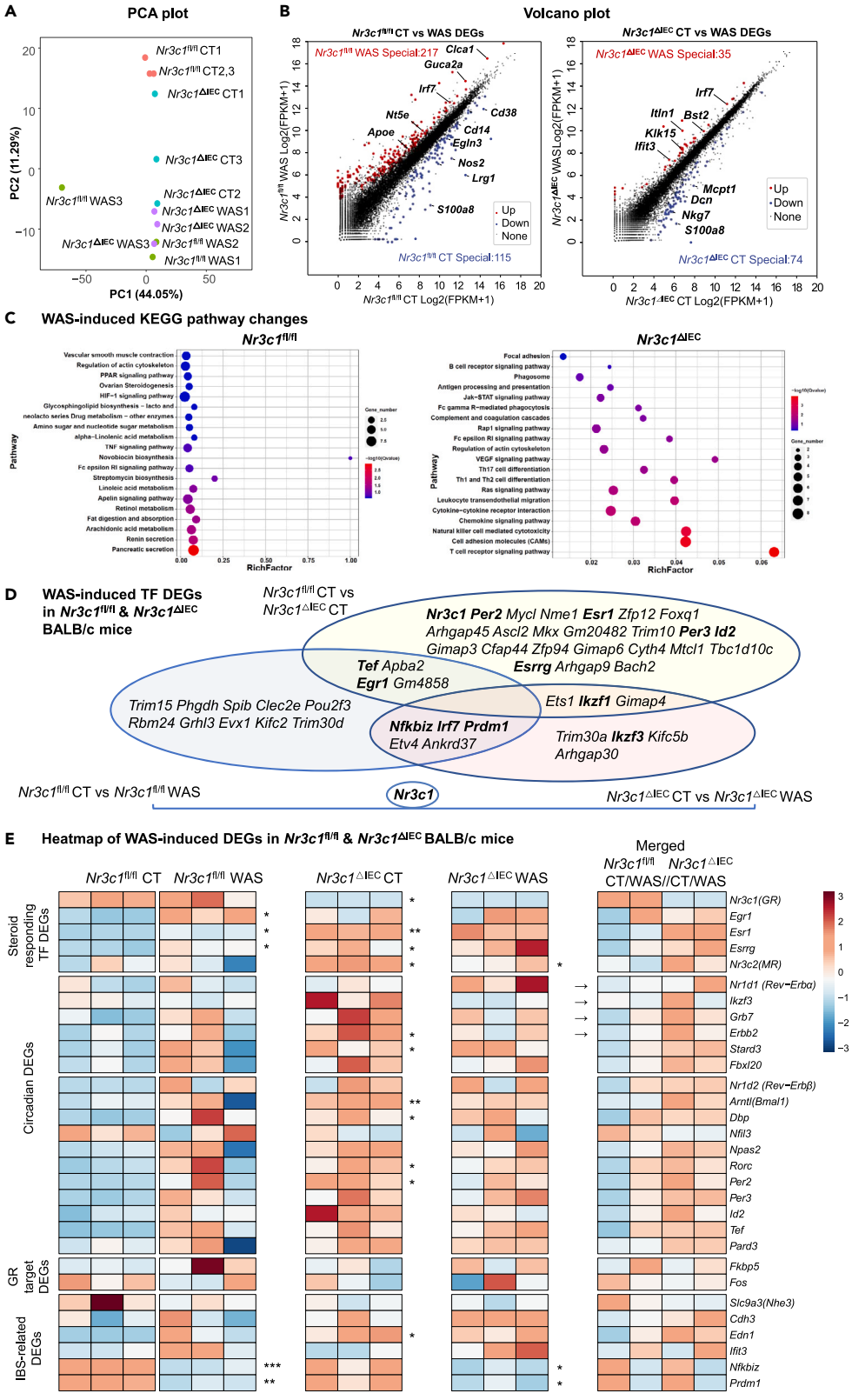
A
PCA plot
PC1 (44.05%)
PC2 (11.29%)
B
Volcano plot
Nr3c1fl/fl CT vs WAS DEGs
Nr3c1fl/fl WAS Special:217
Nr3c1fl/fl CT Special:115
Nr3c1ΔIEC CT vs WAS DEGs
Nr3c1ΔIEC WAS Special:35
Nr3c1ΔIEC CT Special:74
C
WAS-induced KEGG pathway changes
Nr3c1fl/fl
Nr3c1ΔIEC
RichFactor
D
WAS-induced TF DEGs in Nr3c1fl/fl & Nr3c1ΔIEC BALB/c mice
Nr3c1fl/fl CT vs Nr3c1ΔIEC CT
Nr3c1 Per2 Mycl Nme1 Esr1 Zfp12 Foxq1 Arhgap45 Ascl2 Mkx Gm20482 Trim10 Per3 Id2 Gimap3 Cfap44 Zfp94 Gimap6 Cyth4 Mtcl1 Tbc1d10c Esrrg Arhgap9 Bach2
Tef Apba2 Egr1 Gm4858
Trim15 Phgdh Spib Clec2e Pou2f3 Rbm24 Grhl3 Evx1 Kifc2 Trim30d
Ets1 Ikzf1 Gimap4
Nfkbiz Irf7 Prdm1 Etv4 Ankrd37
Trim30a Ikzf3 Kifc5b Arhgap30
Nr3c1fl/fl CT vs Nr3c1fl/fl WAS
Nr3c1
Nr3c1ΔIEC CT vs Nr3c1ΔIEC WAS
E
Heatmap of WAS-induced DEGs in Nr3c1fl/fl & Nr3c1ΔIEC BALB/c mice
Nr3c1fl/fl CT
Nr3c1fl/fl WAS
Nr3c1ΔIEC CT
Nr3c1ΔIEC WAS
Merged
Nr3c1fl/fl Nr3c1ΔIEC CT/WAS//CT/WAS
Steroid responding TF DEGs
Circadian DEGs
GR target DEGs
IBS-related DEGs
Nr3c1(GR)
Egr1
Esr1
Esrrg
Nr3c2(MR)
Nr1d1 (Rev-Erbα)
Ikzf3
Grb7
Erbb2
Stard3
Fbxl20
Nr1d2 (Rev-Erbβ)
Arntl(Bmal1)
Dbp
Nfil3
Npas2
Rorc
Per2
Per3
Id2
Tef
Pard3
Fkbp5
Fos
Slc9a3(Nhe3)
Cdh3
Edn1
Ifit3
Nfkbiz
Prdm1

Figure 6. Intestinal *Nr3c1* deletion altered stress-induced transcriptomic changes

Control (CT) and water avoidance stressed (WAS) *Nr3c1*$^{fl/fl}$ and *Nr3c1*$^{\triangle IEC}$ BALB/c mouse colon epithelium cells were isolated for RNA-seq analysis.

(A) Principal component analysis.

(B) Volcano plot of DEGs.

(C) Intestinal deletion of *Nr3c1* in BALB/c altered KEGG pathway enrichment of WAS-induced DEGs.

(D) Transcription factor DEGs.

(E) Heatmap of steroid responding, circadian, GR target, and IBS-related DEGs. Statistical significance was determined using an unpaired *t* test with Welch's correction (*, $p < 0.05$; **, $p < 0.01$; ***, $p < 0.001$; N = 3).

WAS-induced DEGs in our parallel rat study.[58] Our mouse data unveiled stress-induced remodeling of this chromatin region in 3D (Figure 5E). We detected multiple IBS-related TF DEGs in the *Nr3c1* knockout mice, including *Egr1*, *Nfkbiz*, *Irf7*, *Prdm1*, *Ikzf1*, and *Ikzf3*; suggesting the GR-regulated colon IEC transcription network responsible for IBS (Figure 6).[23,27,28,31,51] Human EGR1 (NGFIA) is responsible for stress-induced *NR3C1* promoter DNA methylation and regulation of IBS-related serotonin synthesis; significant differential expression of *EGR1* is observed in IBS patient biopsies.[4,31,59,60] Mathematicians studied the circadian 4DN to model genomic programming of tissue homeostasis, leading to the proposal of the two-gene (mutual TF inhibition) network "hardwiring."[61] Based on our previous study, we proposed the formation of GR-HES1 pair in the colon crypt axis, and *HES1* was identified as a decreased IBS DEG (IBS-C vs. Healthy Control, $p < 0.0001$; IBS-D vs. Healthy Control, $p < 0.01$).[1,5,29,62] The current study provided evidence of GR-NR1D1 hardwiring in the circadian time axis.[61,62] The colon homeostasis is likely programmed by GR coupled "hardwiring" in time and space.[1,2,61] Finally, these findings support the dynamic synergy between TFs and chromatin looping machinery in stress-GC triggered genomic programming with SNP-determined differences between individuals (Figure S6B).[2,13,20,22]

Information provided in this study has potential applications for developing innovative precision therapy strategies for human bowel disorders (Figures S1 and S6).[2,23,32] BALB/c and C57BL/6J strains have been extensively compared in multiple *in vivo* studies targeting the GBA.[53,63] Intestinal deletion of *Nr3c1* in BALB/c resulted in impaired barrier function previously reported in C57BL/6J; BALB/c *Nr3c1*$^{\triangle IEC}$ mice demonstrated higher stress-induced visceral hyperalgesia than *Nr3c1*$^{fl/fl}$ mice (Figures 7B–7G). The BALB/c strain complemented the C57BL/6J genetic background in this study of *Nr1d1* regulation.[63] The BALB/c *Nr3c1*$^{\triangle IEC}$ mice, which were first generated in this study, may be helpful in further explorations of the GR function. In addition, the BALB/c×C57BL/6J mouse model may elucidate the role of allele-specific gene expression in regulating genome architecture *in vivo* and help develop and validate next-generation pharmacogenomics.[2,53,63] We observed transcriptome differences between WT and *Nr3c1*$^{fl/fl}$ BALB/c mice treated for 5 days with tamoxifen (estrogen analog) before the WAS procedure thus supporting the existence of pharmacological crosstalk that attenuates GC actions. These data indicate that extensive crosstalk between steroids and their nuclear receptors is involved in stress responses (Figures 1F and 6). To represent the full spectrum of patients, datasets generated in females are needed as current datasets are biased toward males. In conclusion, we found GR-mediated *Ikzf3-Nr1d1* 3D chromatin circadian misalignment in a stress-induced IBS animal model, which impaired the circadian transcription regulatory network responsible for intestinal homeostasis. The GR-regulome dataset generated in this study could benefit the development of precision medicine algorithms based on the conserved transcriptional regulation by GR and transcription regulatory enhancer SNPs responsible for IBS (Figure S6).[2,23]

Limitations of the study

Pooled colon IECs in generating the proof-of-concept dataset represent a mixture of different epithelial subtypes. More datasets generated in females are needed to represent the full spectrum of patients.

ETHICS APPROVAL

All experimental procedures were performed following the ethical guidelines of the Animal Management Rules of the Chinese Ministry of Health (Document No.55,2001), and approved by the Animal Care and Use Committee, Union Hospital, Tongji Medical College, HUST, China (Approval ID 2016-0057).

STAR★METHODS

Detailed methods are provided in the online version of this paper and include the following:

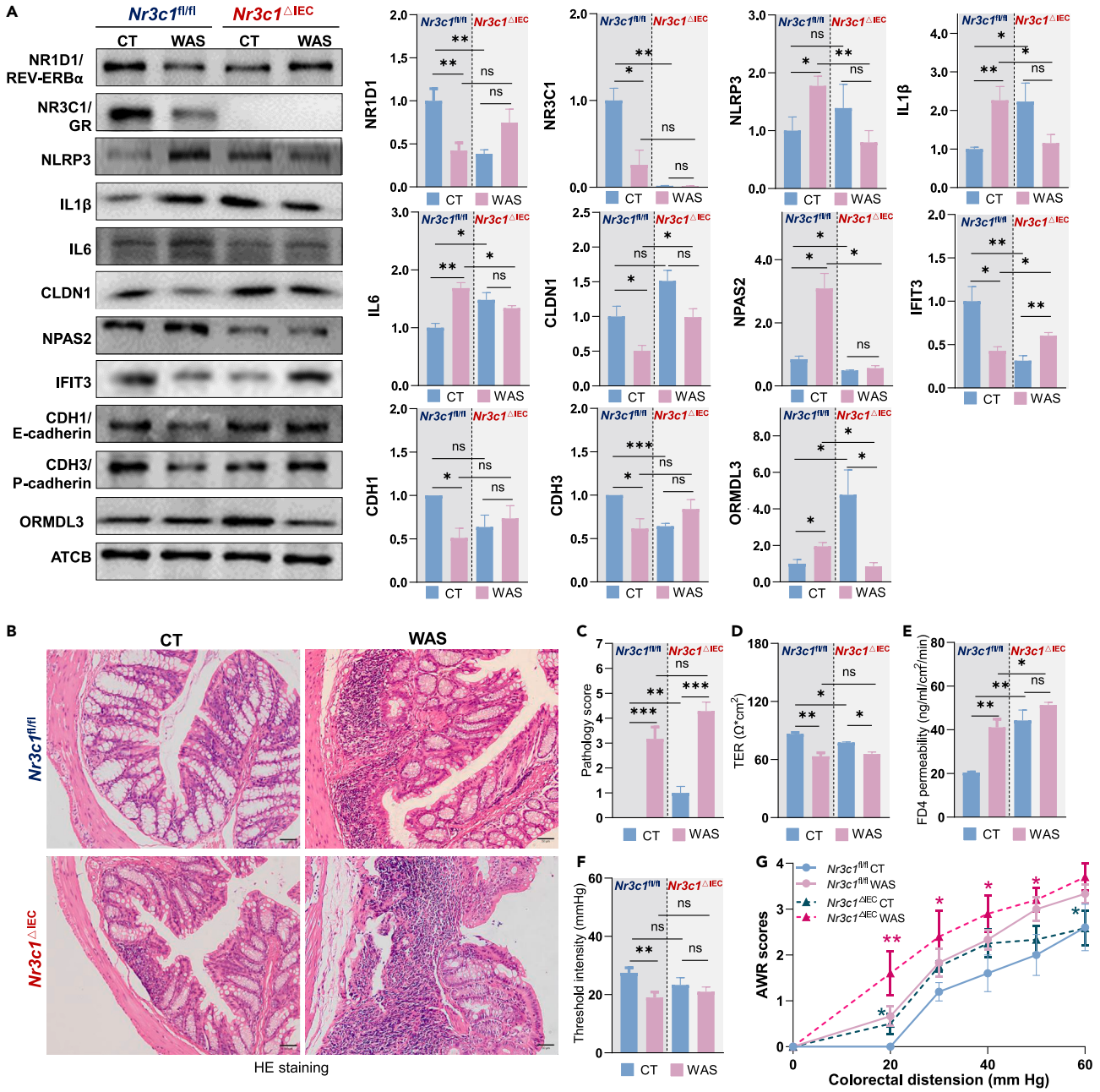

Figure 7. Intestinal *Nr3c1* deletion supported GR's transcriptional regulation of colonic homeostasis

(A) Western blotting analysis of *Nr3c1*$^{fl/fl}$ and *Nr3c1*$^{\triangle IEC}$ BALB/c colon IECs from CT (control) and water avoidance stressed (WAS) groups. *Nr3c1* deletion tended to reverse the WAS-induced changes in protein levels. *Nr3c1* deletion also reduced the significance of stress-induced changes.

(B) Typical hematoxylin-eosin (HE) staining of CT and WAS colon epithelium from *Nr3c1*$^{fl/fl}$ and *Nr3c1*$^{\triangle IEC}$ mice.

(C) Histological scores. *Nr3c1* deletion elevated inflammatory infiltration, while stress enhanced the severity.

(D and E) *Nr3c1* deletion impaired barrier function and reduced the significance of stress-increased permeability; TEER (transepithelial electrical resistance) and FD4 (fluorescein isothiocyanate-dextran 4 kDa) permeability were measured.

(F) Stress reduced the thresholds of pain responses in *Nr3c1*$^{fl/fl}$ mice but not in *Nr3c1*$^{\triangle IEC}$ mice. Data are expressed as means ± standard error. Statistical significance was determined using an unpaired *t* test with Welch's correction (*, $p < 0.05$; **, $p < 0.01$; ***, $p < 0.001$; N = 3, 4, 5).

(G) *Nr3c1* is involved in stress-induced visceral hyperalgesia. AWR (abdominal withdrawal reflex) scores in response to CRD (colorectal distension) were measured. AWR data were analyzed with two-way ANOVA analysis (with Tukey's multiple comparison test); the significance between *Nr3c1*$^{\triangle IEC}$ WAS/*Nr3c1*$^{fl/fl}$ CT and *Nr3c1*$^{\triangle IEC}$ WAS/*Nr3c1*$^{\triangle IEC}$ CT is illustrated (*, $p < 0.05$; **, $p < 0.01$; N = 6).

- KEY RESOURCES TABLE
- RESOURCE AVAILABILITY
  - Lead contact
  - Materials availability
  - Data and code availability
- EXPERIMENTAL MODEL AND SUBJECT DETAILS
  - Animals
  - Colon epithelium cell isolation
  - RNA-seq analysis
  - qPCR analysis
  - Western Blotting
  - Histological analysis
  - Colon permeability assessment
  - CRD and abdominal withdrawal reflex scoring
  - Open-field test
  - CUT&Tag analysis
  - Bisulfite pyrosequencing
  - Cell culture and Luciferase assay
  - BL-Hi-C analysis
- STATISTICAL ANALYSIS

SUPPLEMENTAL INFORMATION

Supplemental information can be found online at https://doi.org/10.1016/j.isci.2023.107137.

ACKNOWLEDGMENTS

This study was supported in part by the National Natural Science Foundation of China (Nos. 82070556, 81770539, 81974068, 81900580). The authors thank Bin Zhang, Hongbo Yang, Fang Hua, and Pingfeng Zhang for insightful discussions. The authors thank Lin Liu and Chenkui Kuang for processing the data.

AUTHOR CONTRIBUTIONS

G.Z., J.W., G.H., R.L., and S.T.Z. conceptualized this study. G.Z., S.Y.P., J.B.W., and F.Y.W. performed animal studies. S.Y.P. validated the animal studies. G.Z., Y.C., D.J.X., M.D.J., Q.W., and L.L.Y. performed BL-Hi-C analysis. D.J.X., J.B.W., and M.D.J. visualized omics data. X.H.H., R.L., and Y.Z. supervised this study. G.Z. wrote the original draft. R.L., J.W., G.H., and Y.Z. reviewed &and edited this manuscript.

DECLARATION OF INTERESTS

The authors declare that they have no competing interests.

Received: January 20, 2023
Revised: April 28, 2023
Accepted: June 12, 2023
Published: June 17, 2023

REFERENCES

1. Mukherji, A., Kobiita, A., Ye, T., and Chambon, P. (2013). Homeostasis in intestinal epithelium is orchestrated by the circadian clock and microbiota cues transduced by TLRs. Cell *153*, 812–827. https://doi.org/10.1016/j.cell.2013.04.020.

2. Wiley, J.W., Higgins, G.A., and Athey, B.D. (2016). Stress and glucocorticoid receptor transcriptional programming in time and space: Implications for the brain-gut axis. Neuro Gastroenterol. Motil. *28*, 12–25. https://doi.org/10.1111/nmo.12706.

3. Wu, W.L., Adame, M.D., Liou, C.W., Barlow, J.T., Lai, T.T., Sharon, G., Schretter, C.E., Needham, B.D., Wang, M.I., Tang, W., et al. (2021). Microbiota regulate social behaviour via stress response neurons in the brain. Nature *595*, 409–414. https://doi.org/10.1038/s41586-021-03669-y.

4. Hong, S., Zheng, G., and Wiley, J.W. (2015). Epigenetic regulation of genes that modulate chronic stress-induced visceral pain in the peripheral nervous system. Gastroenterology *148*, 148–157.e7. https://doi.org/10.1053/j.gastro.2014.09.032.

5. Zheng, G., Victor Fon, G., Meixner, W., Creekmore, A., Zong, Y., K Dame, M., Colacino, J., Dedhia, P.H., Hong, S., and Wiley, J.W. (2017). Chronic stress and intestinal barrier dysfunction: Glucocorticoid receptor and transcription repressor HES1 regulate tight junction protein Claudin-1 promoter. Sci. Rep. *7*, 4502. https://doi.org/10.1038/s41598-017-04755-w.

6. Swan, C., Duroudier, N.P., Campbell, E., Zaitoun, A., Hastings, M., Dukes, G.E., Cox, J., Kelly, F.M., Wilde, J., Lennon, M.G., et al. (2013). Identifying and testing candidate genetic polymorphisms in the irritable bowel

syndrome (IBS): association with TNFSF15 and TNFalpha. Gut *62*, 985–994. https://doi.org/10.1136/gutjnl-2011-301213.

7. Murayama, Y., Yahagi, N., Takeuchi, Y., Aita, Y., Mehrazad Saber, Z., Wada, N., Li, E., Piao, X., Sawada, Y., Shikama, A., et al. (2019). Glucocorticoid receptor suppresses gene expression of Rev-erbalpha (Nr1d1) through interaction with the CLOCK complex. FEBS Lett. *593*, 423–432. https://doi.org/10.1002/1873-3468.13328.

8. Aguilar-Arnal, L., Hakim, O., Patel, V.R., Baldi, P., Hager, G.L., and Sassone-Corsi, P. (2013). Cycles in spatial and temporal chromosomal organization driven by the circadian clock. Nat. Struct. Mol. Biol. *20*, 1206–1213. https://doi.org/10.1038/nsmb.2667.

9. Stokes, K., Cooke, A., Chang, H., Weaver, D.R., Breault, D.T., and Karpowicz, P. (2017). The Circadian Clock Gene BMAL1 Coordinates Intestinal Regeneration. Cell. Mol. Gastroenterol. Hepatol. *4*, 95–114. https://doi.org/10.1016/j.jcmgh.2017.03.011.

10. Thaiss, C.A., Levy, M., Korem, T., Dohnalová, L., Shapiro, H., Jaitin, D.A., David, E., Winter, D.R., Gury-BenAri, M., Tatirovsky, E., et al. (2016). Microbiota Diurnal Rhythmicity Programs Host Transcriptome Oscillations. Cell *167*, 1495–1510.e12. https://doi.org/10.1016/j.cell.2016.11.003.

11. Kim, M.J., Choi, G.E., Chae, C.W., Lim, J.R., Jung, Y.H., Yoon, J.H., Park, J.Y., and Han, H.J. (2023). Melatonin-mediated FKBP4 downregulation protects against stress-induced neuronal mitochondria dysfunctions by blocking nuclear translocation of GR. Cell Death Dis. *14*, 146. https://doi.org/10.1038/s41419-023-05676-5.

12. Fowler, S., Hoedt, E.C., Talley, N.J., Keely, S., and Burns, G.L. (2022). Circadian Rhythms and Melatonin Metabolism in Patients With Disorders of Gut-Brain Interactions. Front. Neurosci. *16*, 825246. https://doi.org/10.3389/fnins.2022.825246.

13. Rinaldi, L., Fettweis, G., Kim, S., Garcia, D.A., Fujiwara, S., Johnson, T.A., Tettey, T.T., Ozbun, L., Pegoraro, G., Puglia, M., et al. (2022). The glucocorticoid receptor associates with the cohesin loader NIPBL to promote long-range gene regulation. Sci. Adv. *8*, eabj8360. https://doi.org/10.1126/sciadv.abj8360.

14. Pacheco-Bernal, I., Becerril-Pérez, F., and Aguilar-Arnal, L. (2019). Circadian rhythms in the three-dimensional genome: implications of chromatin interactions for cyclic transcription. Clin. Epigenetics *11*, 79. https://doi.org/10.1186/s13148-019-0677-2.

15. Kim, Y.H., and Lazar, M.A. (2020). Transcriptional Control of Circadian Rhythms and Metabolism: A Matter of Time and Space. Endocr. Rev. *41*, 707–732. https://doi.org/10.1210/endrev/bnaa014.

16. Wang, S., Lin, Y., Yuan, X., Li, F., Guo, L., and Wu, B. (2018). REV-ERBalpha integrates colon clock with experimental colitis through regulation of NF-kappaB/NLRP3 axis. Nat. Commun. *9*, 4246. https://doi.org/10.1038/s41467-018-06568-5.

17. Scuderi, S.A., Casili, G., Lanza, M., Filippone, A., Paterniti, I., Esposito, E., and Campolo, M. (2020). Modulation of NLRP3 Inflammasome Attenuated Inflammatory Response Associated to Diarrhea-Predominant Irritable Bowel Syndrome. Biomedicines *8*, 519. https://doi.org/10.3390/biomedicines8110519.

18. Okabe, T., Chavan, R., Fonseca Costa, S.S., Brenna, A., Ripperger, J.A., and Albrecht, U. (2016). REV-ERBalpha influences the stability and nuclear localization of the glucocorticoid receptor. J. Cell Sci. *129*, 4143–4154. https://doi.org/10.1242/jcs.190959.

19. Caratti, G., Iqbal, M., Hunter, L., Kim, D., Wang, P., Vonslow, R.M., Begley, N., Tetley, A.J., Woodburn, J.L., Pariollaud, M., et al. (2018). REVERBa couples the circadian clock to hepatic glucocorticoid action. J. Clin. Invest. *128*, 4454–4471. https://doi.org/10.1172/JCI96138.

20. Ramamoorthy, S., and Cidlowski, J.A. (2013). Ligand-induced repression of the glucocorticoid receptor gene is mediated by an NCoR1 repression complex formed by long-range chromatin interactions with intragenic glucocorticoid response elements. Mol. Cell Biol. *33*, 1711–1722. https://doi.org/10.1128/MCB.01151-12.

21. Kim, Y.H., Marhon, S.A., Zhang, Y., Steger, D.J., Won, K.J., and Lazar, M.A. (2018). Rev-erbalpha dynamically modulates chromatin looping to control circadian gene transcription. Science *359*, 1274–1277. https://doi.org/10.1126/science.aao6891.

22. Xu, Y., Guo, W., Li, P., Zhang, Y., Zhao, M., Fan, Z., Zhao, Z., and Yan, J. (2016). Long-Range Chromosome Interactions Mediated by Cohesin Shape Circadian Gene Expression. PLoS Genet. *12*, e1005992. https://doi.org/10.1371/journal.pgen.1005992.

23. Higgins, G.A., Williams, A.M., Ade, A.S., Alam, H.B., and Athey, B.D. (2019). Druggable Transcriptional Networks in the Human Neurogenic Epigenome. Pharmacol. Rev. *71*, 520–538. https://doi.org/10.1124/pr.119.017681.

24. Arloth, J., Bogdan, R., Weber, P., Frishman, G., Menke, A., Wagner, K.V., Balsevich, G., Schmidt, M.V., Karbalai, N., Czamara, D., et al. (2015). Genetic Differences in the Immediate Transcriptome Response to Stress Predict Risk-Related Brain Function and Psychiatric Disorders. Neuron *86*, 1189–1202. https://doi.org/10.1016/j.neuron.2015.05.034.

25. Hu, W., Jiang, C., Kim, M., Yang, W., Zhu, K., Guan, D., Lv, W., Xiao, Y., Wilson, J.R., Rader, D.J., et al. (2021). Individual-specific functional epigenomics reveals genetic determinants of adverse metabolic effects of glucocorticoids. Cell Metab. *33*, 1592–1609.e7. https://doi.org/10.1016/j.cmet.2021.06.004.

26. Chang, L., Di Lorenzo, C., Farrugia, G., Hamilton, F.A., Mawe, G.M., Pasricha, P.J., and Wiley, J.W. (2018). Functional Bowel Disorders: A Roadmap to Guide the Next Generation of Research. Gastroenterology *154*, 723–735. https://doi.org/10.1053/j.gastro.2017.12.010.

27. Camilleri, M., Carlson, P., McKinzie, S., Zucchelli, M., D'Amato, M., Busciglio, I., Burton, D., and Zinsmeister, A.R. (2011). Genetic susceptibility to inflammation and colonic transit in lower functional gastrointestinal disorders: preliminary analysis. Neuro Gastroenterol. Motil. *23*, 935–e398. https://doi.org/10.1111/j.1365-2982.2011.01749.x.

28. Camilleri, M., Carlson, P., Acosta, A., Busciglio, I., Nair, A.A., Gibbons, S.J., Farrugia, G., and Klee, E.W. (2014). RNA sequencing shows transcriptomic changes in rectosigmoid mucosa in patients with irritable bowel syndrome-diarrhea: a pilot case-control study. Am. J. Physiol. Gastrointest. Liver Physiol. *306*, G1089–G1098. https://doi.org/10.1152/ajpgi.00068.2014.

29. Mars, R.A.T., Yang, Y., Ward, T., Houtti, M., Priya, S., Lekatz, H.R., Tang, X., Sun, Z., Kalari, K.R., Korem, T., et al. (2020). Longitudinal Multi-omics Reveals Subset-Specific Mechanisms Underlying Irritable Bowel Syndrome. Cell *182*, 1460–1473.e17. https://doi.org/10.1016/j.cell.2020.08.007.

30. Eijsbouts, C., Zheng, T., Kennedy, N.A., Bonfiglio, F., Anderson, C.A., Moutsianas, L., Holliday, J., Shi, J., Shringarpure, S., 23andMe Research Team, et al.. (2021). Genome-wide analysis of 53,400 people with irritable bowel syndrome highlights shared genetic pathways with mood and anxiety disorders. Nat. Genet. *53*, 1543–1552. https://doi.org/10.1038/s41588-021-00950-8.

31. Camilleri, M., Magnus, Y., Carlson, P., Wang, X.J., Chedid, V., Maselli, D., Taylor, A., McKinzie, S., Kengunte Nagaraj, N., Busciglio, I., and Nair, A. (2022). Differential mRNA expression in ileal and colonic biopsies in irritable bowel syndrome with diarrhea or constipation. Am. J. Physiol. Gastrointest. Liver Physiol. *323*, G88–G101. https://doi.org/10.1152/ajpgi.00063.2022.

32. Higgins, G.A., Hong, S., and Wiley, J.W. (2022). The Role of Epigenomic Regulatory Pathways in the Gut-Brain Axis and Visceral Hyperalgesia. Cell. Mol. Neurobiol. *42*, 361–376. https://doi.org/10.1007/s10571-021-01108-0.

33. Lasconi, C., Pahl, M.C., Cousminer, D.L., Doege, C.A., Chesi, A., Hodge, K.M., Leonard, M.E., Lu, S., Johnson, M.E., Su, C., et al. (2021). Variant-to-Gene-Mapping Analyses Reveal a Role for the Hypothalamus in Genetic Susceptibility to Inflammatory Bowel Disease. Cell. Mol. Gastroenterol. Hepatol. *11*, 667–682. https://doi.org/10.1016/j.jcmgh.2020.10.004.

34. Berce, V., Kozmus, C.E.P., and Potočnik, U. (2013). Association among ORMDL3 gene expression, 17q21 polymorphism and response to treatment with inhaled corticosteroids in children with asthma. Pharmacogenomics J. *13*, 523–529. https://doi.org/10.1038/tpj.2012.36.

35. Chang, M.L., Moussette, S., Gamero-Estevez, E., Gálvez, J.H., Chiwara, V., Gupta, I.R., Ryan, A.K., and Naumova, A.K. (2019). Regulatory

interaction between the ZPBP2-ORMDL3/Zpbp2-Ormdl3 region and the circadian clock. PLoS One *14*, e0223212. https://doi.org/10.1371/journal.pone.0223212.

36. Söderman, J., Berglind, L., and Almer, S. (2015). Gene Expression-Genotype Analysis Implicates GSDMA, GSDMB, and LRRC3C as Contributors to Inflammatory Bowel Disease Susceptibility. BioMed Res. Int. *2015*, 834805. https://doi.org/10.1155/2015/834805.

37. Schmiedel, B.J., Seumois, G., Samaniego-Castruita, D., Cayford, J., Schulten, V., Chavez, L., Ay, F., Sette, A., Peters, B., and Vijayanand, P. (2016). 17q21 asthma-risk variants switch CTCF binding and regulate IL-2 production by T cells. Nat. Commun. *7*, 13426. https://doi.org/10.1038/ncomms13426.

38. Kuang, Z., Wang, Y., Li, Y., Ye, C., Ruhn, K.A., Behrendt, C.L., Olson, E.N., and Hooper, L.V. (2019). The intestinal microbiota programs diurnal rhythms in host metabolism through histone deacetylase 3. Science *365*, 1428–1434. https://doi.org/10.1126/science.aaw3134.

39. Pilz, L.K., Quiles, C.L., Dallegrave, E., Levandovski, R., Hidalgo, M.P.L., and Elisabetsky, E. (2015). Differential susceptibility of BALB/c, C57BL/6N, and CF1 mice to photoperiod changes. Braz. J. Psychiatry. *37*, 185–190. https://doi.org/10.1590/1516-4446-2014-1454.

40. Bishehsari, F., and Keshavarzian, A. (2019). Microbes help to track time. Science *365*, 1379–1380. https://doi.org/10.1126/science.aaz0224.

41. Zhao, H., Sifakis, E.G., Sumida, N., Millán-Ariño, L., Scholz, B.A., Svensson, J.P., Chen, X., Ronnegren, A.L., Mallet de Lima, C.D., Varnoosfaderani, F.S., et al. (2015). PARP1- and CTCF-Mediated Interactions between Active and Repressed Chromatin at the Lamina Promote Oscillating Transcription. Mol. Cell *59*, 984–997. https://doi.org/10.1016/j.molcel.2015.07.019.

42. Furlan-Magaril, M., Ando-Kuri, M., Arzate-Mejía, R.G., Morf, J., Cairns, J., Román-, A., Tenorio-Hernández, L., Poot-Hernández, A.C., Andrews, S., Várnai, C., et al. (2021). The global and promoter-centric 3D genome organization temporally resolved during a circadian cycle. Genome Biol. *22*, 162. https://doi.org/10.1186/s13059-021-02374-3.

43. Markham, A. (2019). Tenapanor: First Approval. Drugs *79*, 1897–1903. https://doi.org/10.1007/s40265-019-01215-9.

44. Stasi, C., Bellini, M., Gambaccini, D., Duranti, E., de Bortoli, N., Fani, B., Albano, E., Russo, S., Sudano, I., Laffi, G., et al. (2017). Neuroendocrine Dysregulation in Irritable Bowel Syndrome Patients: A Pilot Study. J. Neurogastroenterol. Motil. *23*, 428–434. https://doi.org/10.5056/jnm16155.

45. Yu, M., Yang, S., Qiu, Y., Chen, G., Wang, W., Xu, C., Cai, W., Sun, L., Xiao, W., and Yang, H. (2015). Par-3 modulates intestinal epithelial barrier function through regulating intracellular trafficking of occludin and myosin light chain phosphorylation. J. Gastroenterol. *50*, 1103–1113. https://doi.org/10.1007/s00535-015-1066-z.

46. Yu, Y.B., Zuo, X.L., Zhao, Q.J., Chen, F.X., Yang, J., Dong, Y.Y., Wang, P., and Li, Y.Q. (2012). Brain-derived neurotrophic factor contributes to abdominal pain in irritable bowel syndrome. Gut *61*, 685–694. https://doi.org/10.1136/gutjnl-2011-300265.

47. Zimprich, A., Garrett, L., Deussing, J.M., Wotjak, C.T., Fuchs, H., Gailus-Durner, V., de Angelis, M.H., Wurst, W., and Hölter, S.M. (2014). A robust and reliable non-invasive test for stress responsivity in mice. Front. Behav. Neurosci. *8*, 125. https://doi.org/10.3389/fnbeh.2014.00125.

48. Liang, Z., Li, G., Wang, Z., Djekidel, M.N., Li, Y., Qian, M.P., Zhang, M.Q., and Chen, Y. (2017). BL-Hi-C is an efficient and sensitive approach for capturing structural and regulatory chromatin interactions. Nat. Commun. *8*, 1622. https://doi.org/10.1038/s41467-017-01754-3.

49. Smith, S.B., Maixner, W., Palsson, O.S., Van Tilburg, M.A., Kanazawa, M., and Whitehead, W.E. (2014). 584 FKBP5 Gene Is Associated With IBS Diagnosis. Gastroenterology *146*, 109. https://doi.org/10.1016/s0016-5085(14)60392-9.

50. Aranda, C.J., Arredondo-Amador, M., Ocón, B., Lavín, J.L., Aransay, A.M., Martínez-Augustin, O., and de Medina, F.S. (2019). Intestinal epithelial deletion of the glucocorticoid receptor NR3C1 alters expression of inflammatory mediators and barrier function. FASEB J *33*, 14067–14082. https://doi.org/10.1096/fj.201900404RR.

51. Iribarren, C., Nordlander, S., Sundin, J., Isaksson, S., Savolainen, O., Törnblom, H., Magnusson, M.K., Simrén, M., and Öhman, L. (2022). Fecal luminal factors from patients with irritable bowel syndrome induce distinct gene expression of colonoids. Neuro Gastroenterol. Motil. *34*, e14390. https://doi.org/10.1111/nmo.14390.

52. Wiley, J.W., and Chang, L. (2018). Functional Bowel Disorders. Gastroenterology *155*, 1–4. https://doi.org/10.1053/j.gastro.2018.02.014.

53. Watanabe, Y., Arase, S., Nagaoka, N., Kawai, M., and Matsumoto, S. (2016). Chronic Psychological Stress Disrupted the Composition of the Murine Colonic Microbiota and Accelerated a Murine Model of Inflammatory Bowel Disease. PLoS One *11*, e0150559. https://doi.org/10.1371/journal.pone.0150559.

54. Song, G.H., Leng, P.H., Gwee, K.A., Moochhala, S.M., and Ho, K.Y. (2005). Melatonin improves abdominal pain in irritable bowel syndrome patients who have sleep disturbances: a randomised, double blind, placebo controlled study. Gut *54*, 1402–1407. https://doi.org/10.1136/gut.2004.062034.

55. Cai, L., Chen, Q., Yao, Z., Sun, Q., Wu, L., and Ni, Y. (2021). Glucocorticoid receptors involved in melatonin inhibiting cell apoptosis and NLRP3 inflammasome activation caused by bacterial toxin pyocyanin in colon. Free Radic. Biol. Med. *162*, 478–489. https://doi.org/10.1016/j.freeradbiomed.2020.11.003.

56. Arredondo-Hernández, R., Schmulson, M., Orduña, P., López-Leal, G., Zarate, A.M., Alanis-Funes, G., Alcaraz, L.D., Santiago-Cruz, R., Cevallos, M.A., Villa, A.R., et al. (2020). Mucosal Microbiome Profiles Polygenic Irritable Bowel Syndrome in Mestizo Individuals. Front. Cell. Infect. Microbiol. *10*, 72. https://doi.org/10.3389/fcimb.2020.00072.

57. Zhu, S., Min, L., Guo, Q., Li, H., Yu, Y., Zong, Y., Wang, L., Li, P., Gu, J., and Zhang, S. (2018). Transcriptome and methylome profiling in a rat model of irritable bowel syndrome induced by stress. Int. J. Mol. Med. *42*, 2641–2649. https://doi.org/10.3892/ijmm.2018.3823.

58. Wiley, J.W., Higgins, G.A., and Hong, S. (2022). Chronic psychological stress alters gene expression in rat colon epithelial cells promoting chromatin remodeling, barrier dysfunction and inflammation. PeerJ *10*, e13287. https://doi.org/10.7717/peerj.13287.

59. Grasberger, H., Chang, L., Shih, W., Presson, A.P., Sayuk, G.S., Newberry, R.D., Karagiannides, I., Pothoulakis, C., Mayer, E., and Merchant, J.L. (2013). Identification of a functional TPH1 polymorphism associated with irritable bowel syndrome bowel habit subtypes. Am. J. Gastroenterol. *108*, 1766–1774. https://doi.org/10.1038/ajg.2013.304.

60. Meaney, M.J., and Szyf, M. (2005). Environmental programming of stress responses through DNA methylation: life at the interface between a dynamic environment and a fixed genome. Dialogues Clin. Neurosci. *7*, 103–123.

61. Rajapakse, I., and Smale, S. (2017). Emergence of function from coordinated cells in a tissue. Proc. Natl. Acad. Sci. USA *114*, 1462–1467. https://doi.org/10.1073/pnas.1621145114.

62. Zheng, G., Kalinin, A.A., Dinov, I.D., Meixner, W., Zhu, S., and Wiley, J.W. (2018). Hypothesis: Caco-2 cell rotational 3D mechanogenomic turing patterns have clinical implications to colon crypts. J. Cell Mol. Med. *22*, 6380–6385. https://doi.org/10.1111/jcmm.13853.

63. Shimomura, K., Kumar, V., Koike, N., Kim, T.K., Chong, J., Buhr, E.D., Whiteley, A.R., Low, S.S., Omura, C., Fenner, D., et al. (2013). Usf1, a suppressor of the circadian Clock mutant, reveals the nature of the DNA-binding of the CLOCK:BMAL1 complex in mice. Elife *2*, e00426. https://doi.org/10.7554/eLife.00426.

STAR★METHODS

KEY RESOURCES TABLE

REAGENT or RESOURCE	SOURCE	IDENTIFIER
Antibodies		
Glucocorticoid Receptor Rabbit mAb	Cell Signaling Technology	#3660 (D8H2)
Anti-NR1D1 antibody	Abcam	ab174309 [EPR10376]
NLRP3 Rabbit mAb	Cell Signaling Technology	#15101 (D4D8T)
IL1β Rabbit pAb	ABclonal	A16288
IL-6 Rabbit mAb	Cell Signaling Technology	#12912 (D5W4V)
Claudin 1 Monoclonal Antibody	Thermo Fisher	37-4900 (2H10D10)
ORMDL3 Rabbit pAb	ABclonal	A14951
NPAS2 Rabbit pAb	ABclonal	A16930
PARD3 Polyclonal antibody	Proteintech	11085-1-AP
β-Actin Rabbit mAb	ABclonal	AC026
ARNTL Polyclonal antibody	Proteintech	14268-1-AP
Caspase 1/p20/p10 Polyclonal antibody	Proteintech	22915-1-AP
IFIT3 Rabbit pAb	ABclonal	A3924
E-Cadherin Rabbit pAb	ABclonal	A11492
CDH3 Rabbit pAb	ABclonal	A14235
Glucocorticoid Receptor Rabbit mAb	Cell Signaling Technology	#12041 (D6H2L)
Rev-Erbα Rabbit mAb	Cell Signaling Technology	#13418 (E1Y6D)
Chemicals, peptides, and recombinant proteins		
SR9009	MedChemExpress	HY-16989
Fluorescein isothiocyanate–dextran	Sigma-Aldrich	FD4-1G
Insulin	Procell Life Science&Technology	PB180432
Recombinant Murine IFN-γ	PeproTech	315-05
Corticosterone	MedChemExpress	HY-B1618
Mifepristone	MedChemExpress	HY-13683
RPMI 1640	Thermo Fisher	11875093
Fetal Bovine Serum	Thermo Fisher	A4766801
Critical commercial assays		
Dual-Luciferase® Reporter Assay System	Promega	E1910
Deposited data		
IBS colon epithelium transcriptome from water avoidance stressed BALB/c & C57BL/6J mice	https://www.ncbi.nlm.nih.gov/sra	PRJNA792732
GR CUT&Tag analysis of colon epithelium from water avoidance stressed BALB/c mice IBS model	https://www.ncbi.nlm.nih.gov/sra	PRJNA882590
BL-Hi-C analysis of colon epithelium from water avoidance stressed BALB/c mice IBS model	https://submit.ncbi.nlm.nih.gov/geo/	GSE233649
IBS colon epithelium transcriptome from water avoidance stressed floxed and intestinal GR knockout BALB/c mice	https://www.ncbi.nlm.nih.gov/sra	PRJNA884499
Experimental models: cell lines		
YAMC	Wuhan Union Hospital	
Experimental models: organisms/strains		
BALB/c mice	HFK Bioscience	

(*Continued on next page*)

Continued

REAGENT or RESOURCE	SOURCE	IDENTIFIER
BALB/c-*Nr3c1*$^{em1(flox)Smoc}$	Shanghai Model Organisms Center	
BALB/c-*Vil1*$^{em1(2A-CreERT2-SV40poly(A)\ Smoc}$	Shanghai Model Organisms Center	
Oligonucleotides		
Actb qPCR primer	CATTGCTGACAGGATGCAGAAGG/ TGCTGGAAGGTGGACAGTGAGG	
*Nr1d1*qPCR primer	CAGGCTTCCGTGACCTTTCTCA/ TAGGTTGTGCGGCTCAGGAACA	
*Nr1d2*qPCR primer	CAGTGAGAAGCTGAATGCCCTC/ TGCACGGATGAGTGTTTCCTGC	
*Dbp*qPCR primer	ACACCGCTTCTCAGAGGAGGAA/ TCTCGACCTCTTGGCTGCTTCA	
*Cry1*qPCR primer	GGTTGCCTGTTTCCTGACTCGT/ GACAGCCACATCCAACTTCCAG	
Nfil3 qPCR primer	CAGGACTACCAGACATCCAAGG/ AGGACACCTCTGACACATCGGA	
*Npas2*qPCR primer	ACAGCACCACAGCTTTGCCAAG/ CAGCAGGAGTTGCTTTGTGAGG	
*Arntl*qPCR primer	ACCTCGCAGAATGTCACAGGCA/ CTGAACCATCGACTTCGTAGCG	
*Clock*qPCR primer	GGCTGAAAGACGGCGAGAACTT/ GTGCTTCCTTGAGACTCACTGTG	
*Per2*qPCR primer	CTGCTTGTTCCAGGCTGTGGAT/ CTTCTTGTGGATGGCGAGCATC	
Recombinant DNA		
pGL3-Basic	Promega	E1751
Software and algorithms		
Prism 9.0	GraphPad	

RESOURCE AVAILABILITY

Lead contact

Further information and requests for resources and reagents should be directed to lead contact Gen Zheng (zhenggen@hotmail.com).

Materials availability

BALB/c-*Nr3c1*$^{em1(flox)Smoc}$ and BALB/c-*Vil1*$^{em1(2A-CreERT2-SV40poly(A)\ Smoc}$ mice generated in this study will be commercially available from Shanghai Model Organisms Center, Inc.

Data and code availability

Source of the RNA-seq and CUT&Tag data can be accessed from NCBI SRA (https://www.ncbi.nlm.nih.gov/sra) accession PRJNA792732, PRJNA882590, and PRJNA884499; Hi-C data are available from NCBI GEO (https://www.ncbi.nlm.nih.gov/geo/) accession GSE233649.

EXPERIMENTAL MODEL AND SUBJECT DETAILS

Animals

Adult (aged 8 weeks) male BALB/c mice were purchased from HFK Bioscience (Beijing, PRC). All mice were allowed to acclimatize to the animal facility one week after arrival. Mice were group-housed (4/cage) with free access to food and water under a 12:12 h (9 am/9 pm) light-dark cycle in a temperature and humidity-controlled environment. Animals were randomly grouped. Mice were repeatedly exposed to WAS as described previously.[4] The mice were placed on 6×6 cm stainless steel platforms in the middle of tanks filled with water (25°C) to 1 cm

below the height of the platforms. The animals were maintained in the tank for 1 h in the morning (9 am to 10 am) daily for 10 consecutive days. The control mice were kept in standard cages. 50 mg/kg SR9009 (MedChemExpress) was administered to mice via intraperitoneal injection once daily at ZT8.[16]

Flox heterozygous mice (*Nr3c1*$^{flox/+}$) and *Vil1* gene-directed knock-in 2A-CreERT2-polyA heterozygous mice were produced by Shanghai Biomodel Organism Science & Technology Development Co., Ltd. Genomic DNA was isolated from toe biopsies and all offspring were genotyped by PCR. Heterozygous *Nr3c1*$^{flox/+}$ mice were mated with Villin-Cre transgenic mice to generate flox and Cre double-positive heterozygous mice (*Nr3c1*$^{flox/+:\ Cre+}$), which were mated with heterozygous *Nr3c1*$^{flox/+}$ mice to obtain flox homozygous and Cre-positive experimental mice (*Nr3c* $^{flox/flox:\ Cre+}$) and flox homozygous and Cre-negative control mice (*Nr3c1*$^{flox/flox}$), all on a BALB/c background. All mice were injected intraperitoneally with 2 mg tamoxifen (sunflower oil/ethanol mixture, 10:1 v/v) for five consecutive days before the induction of WAS.

Colon epithelium cell isolation

Mice were sacrificed with cervical dislocation after isoflurane anesthesia, and the colons (approximately 0.5–4 cm from the anus/distal and middle colon) were collected, cut open into approximately 5 mm sections, and incubated in Dulbecco's phosphate-buffered saline (DPBS /without Ca^{2+} & Mg^{2+}) containing 8 mM EDTA and 1 mM DTT in 15-ml tubes. After rotation for 75 min at 4°C, the crypts were released and collected by centrifugation at 50 ×*g* for 2 min at 4°C. After a brief wash with ice-cold PBS, the crypts were snap-frozen in liquid nitrogen and stored at -80°C before use. The detailed protocol is available on the TTML website (www.umichttml.org).

The ZT0 time-point was used to minimize the effect of ileal-derived GC on the transcriptional network orchestrated by the circadian clock and microbiota. We used acutely harvested enriched colon epithelial cells to generate transcriptome, GR cistrome, and BL-Hi-C datasets to compare with published human data for conserved genomic mechanisms (Figure S1).

RNA-seq analysis

RNA and DNA were isolated with TIANamp DNA RNA Isolation Kit (Tiangen DP422, Beijing, China) following the manufacturer's instruction and analyzed with Nanodrop (Thermo Fisher) and 2100 Bioanalyzer (Agilent). Biological triplicates were used for every condition. RNA samples were submitted to Wuhan Frasergen Bioinformatics Co., Ltd for RNA-seq analysis.

Library preparation for RNA sequencing. A total amount of 1 μg RNA per sample was used as input material for the RNA sample preparations. Sequencing libraries were generated using NEBNext® UltraTM RNA Library Prep Kit for Illumina® (NEB) following the manufacturer's recommendations, and index codes were added to attribute sequences to each sample. Briefly, mRNA was purified from total RNA using poly-T oligo-attached magnetic beads. Fragmentation was carried out using divalent cations under elevated temperature in NEB Next First Strand Synthesis Reaction Buffer. First-strand cDNA was synthesized using random hexamer primers and M-MuLV Reverse Transcriptase (RNaseH-). Second-strand cDNA synthesis was subsequently performed using DNA Polymerase I and RNase H. Remaining overhangs were converted into blunt ends via exonuclease/polymerase activities. After adenylation of 3' ends of DNA fragments, NEB Next Adaptor with hairpin loop structure was ligated to prepare for hybridization. In order to select cDNA fragments with the right length, the library fragments were purified with the AMPure XP system (Beckman Coulter, Beverly, USA). Then 3 μl uracil-specific excision reagent (USER) Enzyme (NEB) was used with size-selected, adaptor-ligated cDNA at 37°C for 15 min followed by 5 min at 95°C before PCR. Then PCR was performed with Phusion High-Fidelity DNA polymerase, Universal PCR primers, and Index (X) Primer. At last, products were purified (AMPure XP system), and library quality was assessed on the Agilent Bioanalyzer 2100 System.

Clustering and sequencing. The clustering of the index-coded samples was performed on a cBot Cluster Generation System using HiSeq X Ten Cluster Kit (Illumina), following the manufacturer's instructions. After cluster generation, the library preparations were sequenced on an Illumina Nova 6000 platform, and 150 bp paired-end reads were generated.

Sequencing data analysis. Before doing any further analysis, quality control was performed. Software FraserQC (v1.2) was used to do quality control. FraserQC is an in-house software developed by Frasergen Co.Ltd, and analyzed in default parameters. Align reads to the reference genome; we took the mouse

mm10 genome as the reference genome for this project. Sequencing reads were aligned to the reference genome using Tophat2(v2.1.1), Tophat2(v2.1.1) and bowtie2(v2.2.2) in and bowtie2(v2.2.2) in default parameter. Genes and isoforms expression levels are quantified by a software package: RSEM (RNASeq by Expectation-Maximization v1.3.0). RSEM computes maximum likelihood abundance estimates using the Expectation-Maximization (EM) algorithm as its statistical model.

EdgeR (v3.6.8) package method was used for screening differentially expressed genes. EdgeR implements a statistical methodology based on the negative binomial distribution, including empirical Bayes estimation, exact tests, generalized linear models, and quasi-likelihood tests. We screen differentially expressed genes according to the following criteria: Foldchange ≥ 2 and FDR <0.05. KOBAS (v3.0) was used to do pathway enrichment analysis of DEGs. KOBAS 3.0 is a server for gene/protein functional annotation (Annotate module) and functional gene set enrichment (Enrichment module). The Annotate module accepts gene lists as input, including IDs or sequences, and generates annotations for each gene based on multiple databases of pathways, diseases, and Gene Ontology. The Enrichment module accepts either gene list or gene expression data as input and generates enriched pathways, corresponding gene names, *P*-value of enrichment, and enrichment score. Transcription regulators were predicted using the web server BART (Binding Analysis for Regulation of Transcription http://bartweb.org/ version 2.0) with all the DEGs detected above. The top 50 transcription regulators identified with BART were used for predicting the transcription network with the Cytoscape web server (https://cytoscape.org/).

qPCR analysis

qPCR analysis was performed with HiScript III room temperature (RT) SuperMix for qPCR (#R323) and AceQ qPCR SYBR Green Master Mix (#Q111) from Vazyme, PRC. qPCR primer sequences from https://www.origene.com/category/gene-expression/qpcr-primer-pairs were used.

Western Blotting

For immunoblot analysis, isolated colon crypts or YAMC cells scraped off from the dish were lysed with NP40 lysis buffer (50 mmol/L Tris-HCl, 150 mmol/L NaCl, 1% NP40, pH 8.0) supplied with protease inhibitor cocktail (Roche, USA) on ice for 20 min before 5 min 6000 rpm centrifugation at 4°C. Supernatants were collected for SDS-PAGE analysis. The primary antibodies were incubated overnight at 4°C.

Antibodies: GR/NR3C1 (Cell Signaling Technology, Cat.3660, 1:1000), REV-ERBα /NR1D1(Abcam, Cat. ab174309, 1:1000), NLRP3(Cell Signaling Technology, Cat.15101, 1:1000), IL1β(Abclonal, Cat.A16288, 1:1000), IL6 (Cell Signaling Technology, Cat.12912, 1:1000), CLDN1 (Thermo Fisher, Cat.37-4900, 1:10000), ORMDL3 (Abclonal, Cat.A14951, 1:2000), NPAS2 (Abclonal, Cat.A16930, 1:2000), PARD3 (Proteintech, Cat.11085-1-AP, 1:500), ACTB/β-actin (Abclonal, Cat.AC026, 1:10000), BMAL1 (Proteintech, Cat. 14268-1-AP, 1:5000), CLOCK (Abclonal, Cat.A7265, 1:10000), Caspase-1 (Proteintech, Cat.22915-1-AP, 1:1000), IFIT3 (Abclonal, Cat.A3924, 1:1500), CDH1 (Abclonal, Cat.A11492, 1:1500), CDH3 (Abclonal, Cat. A14235, 1:1500).

Histological analysis

For histological analysis, distal colon specimens were fixed in 4% formalin for 24 h and embedded in paraffin, stained with hematoxylin and eosin (H&E). Analysis was then performed by a pathologist blinded to the experimental groupings. The sections were graded as inflammation, crypt injury, and ulceration, as shown in Tab S1; scores were calculated by adding up the score for these grades.

Colon permeability assessment

The colon was removed quickly and flushed with cold Krebs solution (121 mM NaCl, 25 mM $NaHCO_3$, 3.8 mM KCl, 1 mM KH_2PO_4, 1.2 mM $CaCl_2$, 1.2 mM $MgSO_4$, and 11.1 mM glucose). Then each piece was placed into an Ussing chamber (Physiological Instruments, San Diego, CA). The chambers were filled with 5 ml of Krebs solution, maintained at 37°C, and given oxygen throughout the experiment. After a 30 min equilibration period, the spontaneous potential difference and short-circuit current (Isc) in the Ussing chamber were recorded. The transepithelial resistance was calculated using the Acquire and Analyze 2.3 software. 3 ml of FITC-dextran (FD4, 1 mg/ml, Sigma-Aldrich) was added to the mucosal side, and an equal volume of Krebs solution to the other side of each chamber. 100 μl samples were collected and transferred to 96-well plates in duplicate every 30 min. Each sample was checked for FD4 flux at 520 nm with a

fluorescence microplate reader (Molecular Devices, USA). The permeability of each tissue was expressed as the calculated flux of FD4 over 30-60 min.

CRD and abdominal withdrawal reflex scoring

We assessed visceral sensitivity by measuring the behavioral response of the AWR to colorectal distension (CRD). During the test, mice were placed in a restraint container, and they could not escape or turn around. Mice were lightly sedated with halothane, and then a soft latex balloon (1.5 cm long, 1 cm diameter) was inserted into the descending colon 1 cm within the anus. The balloon was secured by tying additional tubing to the mouse tail. The mice were accustomed to this procedure 1 day before the experiment to minimize stress. Firstly, the colorectal balloon was gradually inflated by 5 mm Hg until pain manifested to measure threshold intensity. Then, the balloon was rapidly inflated to constant pressure (20, 30, 40, 50, and 60 mm Hg) to measure the AWR. Two blinded observers observed and measured, and we performed three replicates. The AWR scores were graded on a scale of 0-4: 0, no behavioral response to CRD; 1, brief head movement followed by immobility; 2, contraction of abdominal muscles; 3, lifting of abdomen; 4, body arching and lifting of pelvic structures.[46]

Open-field test

The test mouse was gently placed near the wall side with a length of 50 cm, a width of 50 cm, and a height of 50 cm of the open-field arena and allowed to explore freely for 20 min. The first 10 min were to let the mouse adapt to the environment. Only the last 10 min of the mouse's trajectory was recorded by a video camera and further analyzed with EthoVision XT 13 (Noldus, USA).

CUT&Tag analysis

Equal amounts of colon epithelium cells from four mice were pooled from each group. The CUT&Tag sequencing experiments were performed by Wuhan Frasergen Bioinformatics Co., Ltd. Equal amounts of colon epithelium cells from 4 mice were pooled from each group. Following CUT&Tag analysis was performed by Wuhan Frasergen Bioinformatics Co., Ltd, using an antibody against GR (Cell Signaling, Cat.12041). Isolated colon crypts were fixed with 0.8% formaldehyde in DMEM and quenched with 0.125 M Glycine; then, the nuclei were isolated with 10 mM Tris-HCl pH 8.0, 10 mM NaCl, 0.2% Igepal CA630, protease inhibitors cocktail on ice with 0.5 ml glass grinder. In brief, 10,000-500,000 nuclei were harvested and centrifuged for 3 min at 600×g at RT. Nuclei were washed twice in 100-500 μL Wash Buffer (20 mM HEPES pH 7.5; 150 mM NaCl; 0.5 mM Spermidine; 1× Protease inhibitor cocktail) by gentle pipetting. 10 μL of activated concanavalin A-coated magnetic beads were added per sample and incubated at RT for 10 min. The unbound supernatant was removed, and bead-bound nuclei were resuspended in 50 μL Dig-wash Buffer (20 mM HEPES pH 7.5; 150 mM NaCl; 0.5 mM Spermidine; 1× Protease inhibitor cocktail; 0.05% Digitonin) containing 2 mM EDTA and a 1:50 dilution of the appropriate primary antibody. Primary antibody incubation was performed on a rotating platform for 2 h at RT. Then the liquid was removed from the magnet stand. An appropriate secondary antibody was diluted 1:50 in 50 μL of Dig-Wash buffer, and nuclei were incubated at RT for 1 h. Nuclei were washed using the magnet stand twice for 1 min in 500 μL Dig-Wash buffer to remove unbound antibodies. A 1:200 dilution of pA-Tn5 adapter complex (~0.04 μM) was prepared in Dig-300 Buffer (0.01% Digitonin, 20 mM HEPES, pH 7.5, 300 mM NaCl, 0.5 mM Spermidine, 1× Protease inhibitor cocktail). After removing the liquid, 100 μL was added to the nuclei with gentle vortexing, and incubated with pA-Tn5 at RT for 1 h. Nuclei were washed twice for 1 min in 500 μL Dig-300 Buffer to remove unbound pA-Tn5 protein. Next, nuclei were resuspended in 300 μL tagmentation buffer (10 mM $MgCl_2$ in Dig-300 Buffer) and incubated at 37°C for 1 h. To stop tagmentation, 10 μL of 0.5 M EDTA, 3 μL of 10% SDS, and 2.5 μL of 20 mg/mL Proteinase K were added to 300 μL of the sample, which was incubated at 55°C for 1 h, purified using phenol-chloroform–isoamyl alcohol and ethanol, washed with 100% ethanol and suspended in water. The DNA was amplified by PCR reaction as follows: 3 min at 72°C and 30 s at 98°C followed by 14-20 cycles of 15 s at 98°C and 30 s at 60°C and 30 s at 72°C, with a final extension at 72°C for 3 min. Finally, the amplified DNA was purified using Ampure XP beads (Beckman). Libraries were sequenced on the Illumina Nova-seq platform.

The CUT&Tag pipeline begins with filtering tools (FastQC and Trimmomatic) to remove this interference information, containing adapter sequences, low-quality bases, and undetected bases (indicated by N) in paired-end raw data. After obtaining clean data through quality control, we use Bowtie2 to map clean reads to the reference genome, and further screen out the low-quality mapping, PCR redundancy, and organelle alignment by Samtools and Picard, and thus get the retained valid pairs for subsequent analysis.

Meanwhile, CUT&Tag fragment length distribution is an important index for experiment quality. For this reason, the histograms of the size of the insert are plotted with an R script to check the characteristic peaks, and the results are expected to be like a "wave-shape". Next, we choose MACS2 software based on statistical methods to perform Peak Calling, where the peaks called are significantly enriched regions from retained valid pairs data. For the sequencing experiments with biological replication, the next step is focusing on the reproducibility of the peaks; we compare the two replicate samples to show the overlap between peaks and further evaluate the consistency of peak enrichment multiples. The result of the latter is obtained by a more stringent approach called IDR (Irreproducible Discovery Rate), which is based on the presence or absence of Overlap Peak and considers the consistency of the order of peak enrichment multiples between the two sets of data. After that, the R scripts with Deeptools software are performed to illustrate the signal enrichment analysis of peak regions, gene body regions, and the regions from the TSS (TSS); we also use ChIPseeker to obtain gene annotations on peak regions at the same time. Finally, we visualized the called peaks of all samples using the Integrative Genomic Viewer.

Bisulfite pyrosequencing

Bisulfite pyrosequencing of *Nr1d1* TSS E-box was performed by Sangon Biotech (Shanghai, PRC) Co., Ltd.

Cell culture and Luciferase assay

YAMC cells were grown in RPMI 1640 medium containing 5% FBS (Thermo Fisher, USA), 50 μg/ml gentamicin, 1 μg/ml insulin (Procell), and 0.5 ng/ml murine IFNγ (Peprotech) at 33°C, cells with 95-100% confluency were cultured under the nonpermissive condition (37°C without IFN-ϒ) for 24 h differentiation before treatments. Cells were harvested for western blotting analysis after treatment with 1 μM corticosterone (CORT) (MedChemExpress), 500 nM RU486 (Sigma, USA), 10 μM SR9009 (MedChemExpress), and Vehicle. 3Kb *N1d1* promoter-luciferase plasmids were generated according to published.[16] Mutation of Nr1d1 TSS E-box (**CACGTG**) was conducted with primer: CCTAGCAAACGTGAGAGCTT**AGATTG**ATTGGAGAACTG ACCTCACC, together with its reverse complement. YAMC cells grown at 33°C with 5 U/ml IFN-ϒ with 50% confluency were transfected with plasmids and siRNA with Lipofectamine 3000 (Thermo Fisher) according to the manufacturer's direction, and cells were cultured under the nonpermissive condition 24 h after transfection. Then the transfected cells were harvested for luciferase assay before/after the treatments. Promega (USA) Dual-Luciferase® Reporter system was used to measure the promoter activity.

BL-Hi-C analysis

BL-Hi-C data were generated from colon IEC isolated from two Control (CT) and two WAS model mice. Crosslinked colon epithelium crypts from each mouse were ground in 500 μl nucleus lysis buffer (10 mM Tris-HCl pH 8.0, 10 mM NaCl, 0.2% Igepal CA630, Roche protease inhibitors cocktail) on ice with 0.5 ml glass grinder, and the nuclei were filtered with 40 μm Falcon cell strainer. Then the BL-Hi-C analysis was performed as described previously.[48] Correlations among the four libraries were analyzed with hicrep (https://github.com/TaoYang-dev/hicrep) & hicLibRepeatCor (https://gitlab.com/seqyuan/ctools/-/tree/master/module/CQC/libCor) (Figure S7 and TableS2–S5). Data from each group were combined to achieve higher Hi-C resolution in the subsequent analysis. BL-Hi-C data were visualized with Juicebox. Hi-C figures were generated with Python by Frasergen Bioinformatics Co., Ltd, Wuhan.

STATISTICAL ANALYSIS

GraphPad Prism 9.0 was used for generating figures and statistical analysis. In our hypothesis-driven analysis, the unpaired *t* test with Welch's correction (psychologists' recommended default) was used to examine the mRNA, protein, and luciferase activity quantification data between the 2 groups. Circadian clock gene expression from multiple time points was analyzed with Mann–Whitney test. AWR data were analyzed with two-way ANOVA analysis with Tukey's multiple comparisons. Results were expressed as means ± standard error. $P<0.05$ was considered statistically significant.